No signs of inbreeding despite long term isolation and habitat fragmentation in the critically endangered Montseny brook newt

Valbuena-Ureña E[1,2*], Soler-Membrives A[1*], Steinfartz S[3], Orozco-terWengel P[4], Carranza S[5]

[1]Unitat de Zoologia, Facultat de Biociències, Universitat Autònoma de Barcelona, 08193 Cerdanyola del Vallès (Barcelona), Catalonia, Spain.

[2]Centre de Fauna Salvatge de Torreferrussa (Catalan Wildlife Service – Forestal Catalana). Finca de Torreferrusa, Crta B-140, Km 4,5. 08130, Santa Perpètua de la Mogoda, Barcelona, Spain.

[3]Zoological Institute, Department of Evolutionary Biology, Technische Universität Braunschweig, Mendelssohnstr. 4, 38106 Braunschweig, Germany.

[4]School of Biosciences, Cardiff University, Cardiff, United Kingdom.

[5]Institute of Evolutionary Biology (CSIC-Universitat Pompeu Fabra), Passeig Marítim de la Barceloneta 37-49, 08003 Barcelona, Catalonia, Spain.

Keywords for indexing purposes

Calotriton arnoldi, genetic diversity, population structure, critically endangered, conservation genetics, effective population size

Word counts: 7842

*Corresponding authors

Valbuena-Ureña E

Unitat de Zoologia, Facultat de Biociències, Universitat Autònoma de Barcelona, 08193 Cerdanyola del Vallès (Barcelona), Catalonia, Spain

Emiliojavier.Valbuena@uab.cat

Soler-Membrives A

Unitat de Zoologia, Facultat de Biociències, Universitat Autònoma de Barcelona, 08193 Cerdanyola del Vallès (Barcelona), Catalonia, Spain

Anna.Soler@uab.cat

Running title: Consequences of habitat fragmentation

Abstract

Endemic species with restricted geographic ranges potentially suffer the highest risk of extinction. If these species are further fragmented into genetically isolated subpopulations, the risk of extinction is elevated. Habitat fragmentation is generally considered to have negative effects on species survival, despite some evidence for neutral or even positive effects. Typically, non-negative effects are ignored by conservation biology. The Montseny brook newt (*Calotriton arnoldi*) has one of the smallest distribution ranges of any European amphibian (8 km^2), and is considered critically endangered by the IUCN. Here, we apply molecular markers to analyze its population structure, and find that habitat fragmentation due to a natural barrier has resulted in strong genetic division of populations into two sectors, with no detectable migration between sites. Although effective population size estimates suggest low values for all populations, we found low levels of inbreeding and relatedness between individuals within populations. Moreover, *C. arnoldi* displays similar levels of genetic

47 diversity to its sister species *C. asper*, from which it separated around 1.5 million years
48 ago and which has a much larger distribution range. Our extensive study shows that
49 natural habitat fragmentation does not result in negative genetic effects, such as the loss
50 of genetic diversity and inbreeding on an evolutionary time scale. We hypothesize that
51 species in such conditions may evolve strategies (e.g. special mating preferences) to
52 mitigate the effects of small population sizes. However, it should be stressed that the
53 influence of natural habitat fragmentation on an evolutionary time scale should not be
54 conflated with anthropogenic habitat loss or degradation when considering conservation
55 strategies.

56

57 **Introduction**

58 Among threatened species, those that are endemic to a restricted spatial area should *per*
59 *se* experience a higher risk of extinction. Such risk derives from either stochastic
60 environmental processes (e.g. extreme climatic conditions, fires, etc.), or effects of
61 genetic drift and inbreeding (Allendorf & Luikart 2007). Consequently, the preservation
62 of genetic diversity is important for maintaining the evolutionary (adaptive) potential to
63 overcome environmental changes and enable the population growth and survival that is
64 crucial for the fitness of a species (Allentoft & O'Brien 2010). In general, fragmentation
65 of a species range into smaller subunits by external factors such as anthropogenic
66 activities (Blank *et al.* 2013; Storfer *et al.* 2013) or climatic events (Veith *et al.* 2003)
67 reduces gene flow and compromises the population's long term survival (Sunny *et al.*
68 2014). A central goal of conservation biology is to identify the genetic structure and
69 diversity of species at the population level (Apodaca *et al.* 2012 and references therein),
70 and characterize the gene flow between populations in relation to the species' dispersal

propensity (i.e. the probability of dispersal between habitat patches) and rates (Slatkin 1994). Organisms with lower dispersal rates are more susceptible to isolation than those with higher dispersal rates. Thus, dispersal may counteract the loss of gene flow among populations and, therefore, has been shown to be an important factor for the long-term survival of species (Allentoft & O'Brien 2010).

Strong genetic differentiation among populations is a sign of interrupted gene flow, with non-natural external factors such as human-induced disturbance causing habitat fragmentation and hindering dispersal (Templeton *et al*. 1990). However, strong differentiation can also be the outcome of non-human mediated processes, such as naturally occurring habitat fragmentation, local adaptation (e.g. Nosil *et al*. 2009; Steinfartz *et al.* 2007) or incipient speciation on a small spatial scale (e.g. MacLeod *et al*. 2015). While it has been generally argued that fragmentation can lead to isolation and thus increase extinction risks, it has also been suggested that in some instances habitat fragmentation can have neutral or even positive effects (Fahrig 2003). A fragmented species may develop populations which individually harbor low levels of genetic variation, but when all populations are considered together, the species does not present low levels of diversity. Consequently, fragmented species may preserve high levels of total genetic variation, similar to equally sized species with panmitic population (Templeton *et al.* 1990).

Amphibians are generally considered to have limited dispersal abilities, causing genetic differentiation across small geographic scales (Monsen & Blouin 2004 and references therein), although more recent studies indicate that in some cases, dispersal propensities have been vastly underestimated (e.g. Smith & Green 2005). The notable sensitivity of amphibians to environmental change and habitat fragmentation are other factors that may reinforce patterns of sharp genetic discontinuation over short distances

(Savage *et al.* 2010; Storfer *et al.* 2013; Velo-Antón *et al.* 2013). Therefore, data on gene flow between populations of endangered amphibians should have a direct influence on management programs and decisions regarding conservation strategies, such as determining the number of breeding lines and translocation actions (Sunny *et al.* 2014).

The genus *Calotriton* (Gray, 1858 and recently resurrected by Carranza & Amat 2005), includes only two species, both inhabiting the Iberian Peninsula and adapted to live in cold and permanent-flowing streams: the Pyrenean brook newt (*C. asper*) and the Montseny brook newt (*C. arnoldi*). *Calotriton asper* is widely distributed across the Pyrenean mountain chain, with some populations extending northwards and southwards, reaching the Pre-Pyrenees, and occupying an area larger than 20,000 km^2. In contrast, *C. arnoldi* is only known from the Montseny Natural Park in the NE Iberian Peninsula, and its disconnected populations are found within a restricted altitudinal range in seven geographically proximate brooks. Although the historic range of this species is unknown, it currently occupies a total area of only 8 km^2. Moreover, its habitat is naturally fragmented into two watersheds, on the eastern and western sectors of the Tordera River valley, separated by unsuitable terrestrial habitat between them (see Figure 1A). The current census population size of this species is estimated to be less than 1,500 adult individuals (Carranza & Martínez-Solano 2009). Additionally, recent human activities (e.g. extraction of large amounts of water for commercial purposes, deforestation and the building of forest tracks and roads) have had a significant negative effect on *C. arnoldi*'s habitat (Amat *et al*. 2014). Hence, *C. arnoldi* is among of the most spatially restricted and endangered vertebrates in Europe, and it is classified as critically endangered by the International Union for Conservation of Nature (IUCN) (Carranza & Martínez-Solano 2009).

A previous study based on mitochondrial (Cyt *b*) and nuclear (RAG-1) sequences, as well as morphological characters suggested a high degree of differentiation between populations in the eastern and western sectors of *C. arnoldi*'s distribution range (Valbuena-Ureña *et al.* 2013). Therefore, the observed fragmentation of this species into highly genetically isolated populations is probably the result of an ancient, naturally driven, intrinsic fragmentation process rather than the result of recent human disturbances. However, a detailed exploration of population structure, gene flow among populations, and estimates of ancient and current effective population sizes is lacking. Such studies are crucial for the understanding of past and ongoing evolutionary processes, and their implications for the conservation of such a spatially restricted endemic species.

Although there exists several studies of species with very limited distribution ranges (e.g. Sunny *et al.* 2014), as well as of amphibians with highly structured populations (Blank *et al.* 2013; Blouin *et al.* 2010; Monsen & Blouin 2004; Savage *et al.* 2010), *C. arnoldi* represents an exceptional example of a critically endangered amphibian species with limited dispersal capabilities inhabiting a very small fragmented habitat. Here, we present an analysis of the genetic diversity and evolutionary history of *C. arnoldi* which provides general insights into management priorities of species with a very limited distribution range. In order to estimate the effects of natural habitat fragmentation for this species in terms of fitness related genetic parameters (e.g. genetic diversity, inbreeding coefficients, etc.), we compared these parameters directly in populations from the non-fragmented range of sister species *C. asper* in the central Pyrenees. We discuss the absence of anticipated negative consequences for these parameters in *C. arnoldi* in the light of species conservation in naturally fragmented species.

Material and methods

Sampling and DNA extraction

A total of 160 adult *C. arnoldi* were analyzed, including samples from all seven known locations of this species (Figure 1A). In recognition of the low dispersal capacity (Carranza & Martínez-Solano 2009) and the absence of migrants between sites (see Results below), individuals from the seven locations are considered herein as demographic populations. Genetic populations will be referred to henceforth as clusters. For conservation reasons, the three eastern populations are herein referred to as A1, A2, A3, and the four western populations as B1, B2, B3 and B4. Samples included 77 individuals from the eastern sector (23 from A1, and 27 from each A2 and A3 populations) and 83 individuals from the western sector (25 from B1, 28 from B2, 26 from B3 and 4 from B4). The small number of individuals from B4 is due to the low abundance of individuals at this site. Therefore, results from this population should be treated with caution. Tissue samples consisted of small tail or toe clips preserved in absolute ethanol. Genomic DNA was extracted using the QiagenTM (Valencia, California) DNeasy Blood and Tissue Kit, following the manufacturer's protocol.

Phylogenetic analyses and estimation of divergence times

A dataset of mitochondrial and nuclear genes was assembled to estimate the divergence times between *C. asper* and *C. arnoldi,* as well as between *C. arnoldi*'s populations. This dataset consisted of three samples of *C. asper* form Irati, northwestern Pyrenees,

169 Spain (see Milá *et al*. 2010), and a randomly selected set of three samples from each of
170 the seven known wild populations of *C. arnoldi* (Figure 1A, Supplementary Table S1).
171 The following regions of four mitochondrial and three nuclear genes were amplified and
172 sequenced for both strands, totaling 3553 base pairs (bp) (84 variable positions): 374 bp
173 (16 variable) of the mtDNA gene cytochrome *b* (Cyt *b*) using primers Cytb1EuprF and
174 Cytb2EuprR from Carranza & Amat (2005) and conditions as in Carranza *et al.* (2000);
175 556 bp (42 variable) of the mtDNA gene NADH dehydrogenase subunit 4 (ND4) using
176 primers from Arèvalo *et al.* (1994) and conditions as in Martínez-Solano *et al.* (2006);
177 370 bp (5 variable) of the mtDNA gene 12S rRNA (12S) and 553 bp (5 variable) of the
178 mtDNA gene 16S rRNA (16S) with the same primers and conditions as in Carranza &
179 Amat (2005); 695 bp (7 variable) of the nucDNA gene proopiomelanocortin (POMC)
180 and 475 bp (3 variable) of the nucDNA gene brain-derived neurotrophic factor (BDNF)
181 using primers and conditions as in Recuero *et al.* (2012); and 530 bp (6 variable) of the
182 nucDNA gene recombination-activating gene 1 (RAG-1) with primers and conditions as
183 in Šmíd *et al.* (2013). GENEIOUS v. R6.1.6 (Biomatters Ltd.) was used for assembling
184 and editing the chromatographs. Heterozygous positions for the nuclear coding gene
185 fragments were identified based on the presence of two peaks of approximately equal
186 height at a single nucleotide site in both strands, and were coded using IUPAC
187 ambiguity codes. The nuclear coding fragments were translated into amino acids and no
188 stop codons were observed. DNA sequences were aligned for each gene independently
189 using the online application of MAFFT v.7 (Katoh & Standley 2013) with default
190 parameters (Auto strategy, Gap opening penalty: 1.53, Offset value: 0.0). In order to
191 optimize the alignment of the ribosomal genes, we did not include any outgroups and
192 used Bayesian methods for inferring the root of the phylogenetic tree (Huelsenbeck *et*
193 *al.* 2002).

194 Best-fitting models of nucleotide evolution were inferred using jModeltest
195 v.0.1.1 (Darriba *et al.* 2012) under the Akaike information criterion (AIC) (Akaike
196 1973). The HKY model was selected for the 12S and 16S genes and the TrN for all the
197 remaining genes. Phylogenetic analyses were performed using BEAST v.1.8.0
198 (Drummond & Rambaut 2007). For the time calibration, we used the Hauswaldt *et al*.
199 (2014) rate of molecular evolution of the Cyt *b* gene, inferred for the Urodelan genus
200 *Salamandrina*, based on four fossil/geological calibration points. Three individual runs
201 of $5x10^7$ generations were performed, sampling every 10,000 generations. Models and
202 prior specifications applied were either program defaults or as follows: model of
203 sequence evolution for each gene, as indicated above; substitution models and clock
204 models unlinked; trees linked; coalescent constant size tree prior; random starting tree;
205 strict clock rate for all the partitions. The molecular evolution rate of Hauswaldt *et al*.
206 (2014) was implemented in our analyses in the clock rate prior of Cyt *b* using a Normal
207 distribution centered at 0.0102 subst/site/Myr, and with a standard deviation that
208 captured 95% of the High Probability Density of the posterior reported by Hauswaldt *et*
209 *al*. (2014) (0.0085 – 0.018 subst/site/Myr). Posterior trace plots and effective sample
210 sizes (ESS) of the runs were monitored in Tracer v1.5 (Rambaut & Drummond 2007) to
211 ensure convergence. The results of the individual runs were combined in LogCombiner,
212 discarding the initial 10% of the samples, and the maximum clade credibility (MCC)
213 ultrametric tree was produced with TreeAnnotator (both provided with the BEAST
214 package). Nodes were considered strongly supported if they received posterior
215 probability (pp) support values ≥ 0.95.

216

217 *Microsatellite loci genotyping and basic population genetic parameters*

Individuals were genotyped for a total set of 24 microsatellite loci: 15 specifically developed for *C. arnoldi* (Valbuena-Ureña *et al.* 2014) and nine additional loci originally developed for the closely related sister species *C. asper*, and which cross-amplify successfully in *C. arnoldi* (Drechsler *et al.* 2013). Microsatellite loci were multiplexed in five mixes using the Type-it multiplex PCR (Qiagen). Primer combinations of the five mixes are provided in the supplementary material (Supplementary Table S2). PCR conditions and genotyping of loci followed the descriptions provided in Drechsler *et al*. (2013).

The MICRO-CHECKER software (Van Oosterhout *et al.* 2004) was used to check for potential scoring errors, large allele dropout and the presence of null alleles. Pairwise linkage disequilibrium between loci was checked using the software GENEPOP version 4.2.1 (Rousset 2008). The same program was used to calculate deviations from Hardy-Weinberg equilibrium in each population and for each locus, which provides an exact probability value (Guo & Thompson 1992). Genetic diversity was measured for each sampling site as the mean number of alleles (A), observed (H_O) and expected heterozygosity (H_E) and allelic richness (Ar) using FSTAT version 2.9.3.2 (Goudet 1995). The observed number of private alleles for each locus and each population was calculated with GDA (Lewis & Zaykin 2000), and a rarified measure of private allele richness (PAAr) was obtained with HP-RARE (Kalinowski 2005). FSTAT was used to estimate the populations' inbreeding coefficients (F_{IS}) following Weir & Cockerham (1984).

In order to compare the genetic diversity measures of *C. arnoldi* to its more widely distributed sister species in the central Pyrenees, we used four *C. asper* populations from the study of Drechsler *et al.* (2013) (Figure 1A) as a reference, adding some samples and re-sequencing others for some markers (see Suplementary Table S2).

243 The genetic diversity estimates in terms of differences in heterozygosity estimates (H_E
244 and H_O) and number of alleles per locus (A) between *C. arnoldi* populations (and
245 clusters) and these four populations of *C. asper* were tested pairwise using a
246 nonparametric Wilcoxon signed-rank test, with Bonferroni's correction for multiple
247 comparisons. The inbreeding coefficients F_{IS} were also estimated for the *C. asper*
248 populations.

249

250 *Microsatellite-loci derived population structure analysis*

251 The pairwise population divergence between *C. arnoldi*'s seven sampling localities was
252 estimated with the F_{ST} as calculated in FSTAT, and with Jost's D (Jost 2008) using the
253 R package DEMEtics (Gerlach *et al.* 2010). We also used a Bayesian approach to
254 examine population structure of *C. arnoldi* across its distribution range, as implemented
255 in STRUCTURE version 2.3.4 (Pritchard *et al.* 2000). STRUCTURE's Bayesian
256 clustering algorithm assigns individuals to clusters without using prior information on
257 their localities of origin. Settings used included an admixture model with correlated
258 allele frequencies, and the number of inferred clusters (*K*) ranged from one (complete
259 panmixia) to eight (i.e. the number of sample locations plus one). STRUCTURE was
260 run for each value of *K* ten times, with one million Markov Chain Monte Carlo
261 (MCMC) iterations, discarding the first 100,000 MCMC steps as burn-in phase. We also
262 ran STRUCTURE with the same parameters for each sector (eastern and western)
263 separately to check for possible genetic substructure within sectors. The optimal number
264 of clusters was inferred using Evanno *et al.* (2005) ΔK method, as implemented in
265 STRUCTURE HARVESTER (Earl & vonHoldt 2012). The average from all the outputs
266 of each *K* was obtained with CLUMPP version 1.1.2 (Jakobsson & Rosenberg 2007)

and plotted with DISTRUCT version 1.1 (Rosenberg 2004). Additionally, we employed a model-independent clustering approach using GENETIX, version 4.05.2 (Belkhir *et al.* 2004), by performing a factorial correspondence analysis (FCA) on the allelic frequencies obtained for the seven Montseny brook newt populations. This analysis was performed across the distribution range of *C. arnoldi*, as well as in each sector separately to examine the existence of substructure within them. Analysis of molecular variance (AMOVA) was performed in ARLEQUIN 3.5.1.2 (Excoffier & Lischer 2010) by grouping the sampling localities as indicated by STRUCTURE. Isolation by distance (IBD) was evaluated by examining the relationship between geographical and genetic distances between populations with a Mantel test (Mantel 1967). Since the lifestyle of *C. arnoldi* is strictly aquatic (Carranza & Amat 2005), geographic distances were calculated following the watercourse and log-transformed to linearize the relationship between geographic distances and F_{ST} values (see Rousset 1997). Genetic distances were calculated as F_{ST} /(1- F_{ST}), and the significance of matrix correlation coefficients was estimated with 2,000 permutations in ARLEQUIN. Analyses were performed between all sampled populations and by grouping populations by sector using ARLEQUIN.

Analysis of recent gene flow

Recent gene flow between sectors and populations within sectors were assessed using three programs: GENECLASS 2.0 (Piry *et al.* 2004), STRUCTURE and BIMr (Faubet & Gaggiotti 2008). The Bayesian assignment approach implemented in GENECLASS was used following Paetkau *et al*. (2004). STRUCTURE was rerun to detect migrants by calculating a *Q* value, which is the proportion of that individual's ancestry from a

population. An individual is a putative migrant when the Q value for its origin site (Q_o) is lower than the Q value for its site of assignment (Q_a). BIMr was used to estimate migration rates within the last two generations ($N_{gen} \leq 2$) between populations within sectors. BIMr uses a Bayesian assignment test algorithm to estimate the proportion of genes derived from migrants within the last generation, assuming linkage equilibrium and allowing for deviation from Hardy-Weinberg equilibrium. We estimated migration rates among populations within sectors separately. For each analysis, we ran a Markov chain with a burn-in period of 50,000 iterations, followed by 50,000 samples which were collected using a thinning interval of 50. Convergence of the Markov Chain was assessed by repeating the analyses independently five times. Pairwise migration rates between and within populations across runs were averaged.

Inference of demographic history

The effective population size (N_e) for each *C. arnoldi* population and cluster resulting from STRUCTURE, and for the four *C. asper* populations, were calculated using three single-sample N_e estimators: ONeSAMP (Tallmon *et al.* 2008), COLONY version 2.0.4.4 (Jones & Wang 2010), and LDNe version 1.31 (Waples & Do 2008). ONeSAMP employs approximate Bayesian computation (ABC) and calculates eight summary statistics to estimate N_e from a sample of microsatellite loci genotypes. The analyses were submitted online to the ONeSAMP 1.2 server (http://genomics.jun.alaska.edu/asp/Default.aspx). A variety of input priors were tested, with minimum N_e as low as 2 and maximum N_e as high as 1000. After convergence of test runs was achieved, the prior distributions were set between a minimum N_e of 2 and a maximum value of 100 for populations or 500 for clusters. COLONY implements a

315 maximum likelihood method to conduct sibship assignment analyses, which are used to
316 estimate N_e under the assumption of random mating. COLONY was run using the
317 maximum likelihood approach for a dioceous/diploid species, with medium length runs
318 and random mating, assuming polygamy for both males and females (as is the case for
319 most salamanders) with no sibship prior. We did not use the option "update allelic
320 frequencies" and other parameters used as default. Finally, LDNe employs a linkage
321 disequilibrium method (Hill 1981) using a jackknife approach to estimate confidence
322 intervals, and assuming a minimum allele frequency of 2% in order to reduce the bias
323 caused by rare alleles.

324 In order to characterize changes in demographic, history, additional analysis was
325 performed in MSVAR version 1.3 (Storz & Beaumont 2002). This analysis was
326 undertaken for all populations with the exception of B4, due to the low sample size.
327 MSVAR uses a Bayesian approach with coalescent simulations to estimate three
328 population demographic parameters: i) the ancestral population size (N_t) of a
329 population, ii) its current effective population size (N_0), and iii) the time (t) at which the
330 change from N_t to N_0 occurred. Three scenarios, a bottleneck, an expansion and a stable
331 demography, were tested for each population in order to assess whether the posterior
332 distributions of the three parameters of interest were independent of the prior
333 distributions used to run the analyses. As no microsatellite mutation rate for this species
334 has been described, an average vertebrate rate of 10^{-4} was used (Bulut *et al.* 2009),
335 allowing the rate to vary by up to two orders of magnitude above (10^{-2}) and below (10^{-6}). Prior distributions are shown in supplementary information (Supplementary Table
337 S3). Each MSVAR run consisted of $4x10^8$ iterations of the MCMC algorithm,
338 discarding the first 25% of the coalescent simulations. Gelman and Rubin's diagnostic
339 (Brooks & Gelman 1998) was used to asses convergence between the independent

MSVAR runs using the library CODA (Plummer *et al.* 2006) in R. Lastly, the demographic analysis with MSVAR was complimented with bottleneck analyses in Bottleneck v1.2.02 (Piry *et al*. 1999), under the stepwise mutation and the two-phased mutation models with default parameters.

Genetic relatedness of individuals

In order to measure levels of inbreeding, the software MLRELATE (Kalinowski *et al.* 2006) was used, which estimates the relatedness among individuals within each population. This program is appropriate as it is designed for microsatellite loci, is based on maximum likelihood tests, and considers null alleles. Furthermore, GenAlEx v. 6 (Peakall & Smouse 2006) was used to obtain pairwise relatedness among individuals in each population separately using the r_{qg} estimator (Queller & Goodnight 1989). Mean pairwise relatedness values and their 95% confidence intervals estimates (CI) were calculated for the east and west sectors separately, and the statistical differences in mean population-relatedness between populations were assessed with a permutation test following Peakall & Smouse (2006). These CI intervals of r_{qg} from the simulations represent the range of r_{qg} that would be expected under random mating across all populations within sectors. Population r_{qg} values that fell above the expected 95% CI values indicate a higher relatedness than anticipated and are possibly due to reproductive skew, inbreeding, or genetic drift among populations within the same sector. These estimates of genetic relatedness were also computed for the four *C. asper* populations and are used as a reference of non-fragmented populations.

Results

364 *Estimation of divergence times*

365 Convergence was confirmed by examining the likelihood and posterior trace plots of the
366 three runs with Tracer v.1.5. Effective sample sizes of the parameters were above 200,
367 indicating a good representation of independent samples in the posterior. The
368 phylogenetic relationships are shown in Figure 1B. *Calotriton asper* and *C. arnoldi*
369 form two independent clades, and within *C. arnoldi* there are two well supported
370 reciprocally monophyletic groups that include the populations from the eastern and
371 western sectors. Nevertheless, none of the sampling localities within either of the two
372 sectors were monophyletic, likely indicating a lack of resolution of the gene fragments
373 used, and/or gene flow between the localities in each sector, or the retention of ancestral
374 polymorphisms between sectors. According to the present dating estimates, *C. asper*
375 and *C. arnoldi* diverged approximately 1.76 Mya (95% HPD 1.24 – 2.44 Ma) and the
376 eastern and western sectors of *C. arnoldi* 0.18 Mya (95% HPD 0.08 – 0.30 Ma).

377

378 *Genetic diversity*

379 Genetic diversity for each sampled population and cluster obtained from the genetic
380 structure analyses are given in Table 1 (Supplementary Table S4, for locus-specific
381 results). Loci Us3 and Us7 were monomorphic for the populations within the western
382 sector. We further found that some alleles were fixed for some populations:
383 Calarn15906 was found to be monomorphic in population B2, seven loci (Calarn 29994,
384 Calarn06881, Calarn36791, Calarn52354, Calarn31321, Calarn15136 and Us2) were
385 fixed in population B3, and loci Calarn15906 and Ca32 showed no polymorphisms for
386 individuals of population B4. The observed number of alleles per locus ranged from
387 four to 12, with a mean of 7.08, and the mean number of alleles in the eastern and

388 western populations were 5.50 and 3.96, respectively. There was no sign of linkage
389 disequilibrium between any pair of loci, with the only exception of Calarn02248 and
390 Calarn50748 in population B3 after Bonferroni correction (P<0.00018). Only two loci
391 in two different populations showed signs of null alleles (Us7 in A1 and Ca22 in B1).
392 Private alleles (PA) – defined here as alleles exclusively found in a single population
393 throughout the study site, i.e. the species range – are also listed in Table 1. Populations
394 of the eastern sector had 75 PAs, while the western populations had 38 PAs. Allelic
395 richness (AR) per population ranged from 1.77 to 4.22, and expected heterozygosity
396 ranged from 0.197 to 0.559 (weighted average: 0.441), with the lowest value found in
397 B3 and the highest in A3. No significant departures from Hardy-Weinberg equilibrium
398 (P>0.0003) were found after applying Bonferroni correction. Overall, F_{IS} was estimated
399 to be 0.380 (P=0.0021), but this parameter did not show values significantly different
400 from zero for each population after applying Bonferroni correction (see Table 1).

401 Similar levels of genetic diversity were observed between *C. arnoldi* populations
402 or clusters and the four *C. asper* populations (Table 1, Supplementary Table S5). None
403 of the F_{IS} values were significantly different from zero for these four populations after
404 applying Bonferroni correction. In general, the total number of alleles per locus and
405 expected and observed heterozygosity values were similar between *C. asper* and *C.*
406 *arnoldi* populations (and clusters). The differences detected in the western sector are
407 mostly due to population B3, which has low levels of genetic diversity. This population
408 showed some significant differences, mainly when compared to *C. asper* populations at
409 Barranco de Valdragás and Ibón de Acherito (Supplementary Table S6). We only found
410 differences in one of the diversity indices explored (A) with two populations (B2 and
411 B4) compared to two out of the four C. asper populations. We did not detect differences

412 in terms of expected nor observed heterozygosities between any *C. arnoldi* and *C. asper*
413 populations but population B3.

414

415 *Determining population structure*

416 Population differentiation was significant for each pair of population combinations
417 (P<0.001) for both the F_{ST} and Jost's D (Table 2). F_{ST} values between the eastern *versus*
418 western sector populations ranged from 0.443 to 0.617, and Jost's D values from 0.801
419 to 0.877. Pairwise comparisons between populations within sectors were much lower,
420 with F_{ST} and D values within sectors ranging from 0.086 to 0.372 and 0.100 to 0.299,
421 respectively. Population B4 was not included in the F_{ST} and D estimations due to its low
422 sample size. Populations A3 of the eastern and B3 of the western sector were the most
423 differentiated populations when compared with their respective sector populations.

424 Consistent with the results of phylogenetic analyses, STRUCTURE revealed two
425 highly distinct genetic clusters corresponding to populations constituting the eastern and
426 the western sectors (Figure 2). The existence of two clusters was highly supported by
427 the analysis of ΔK values corresponding to K = 2 (Figure 2B). Some evidence for
428 additional substructure is also indicated by a second weak peak at K = 4. When each
429 sector was analyzed independently, two clusters were further identified in each sector,
430 grouping A3 separately from A1 and A2, and B3 separately from B1, B2 and B4
431 (Figure 2A). The same general results were also found with the FCA (Supplementary
432 Figure S1), which demonstrated the clear separation between the two sectors. In these
433 results, A3 and B3 were also the most distinct populations in their respective sectors.
434 The results of the *a posteriori* AMOVA revealed that the clusters resulting from
435 STRUCTURE (K=2) explained 40.81% of the molecular variance, 11.61% was

436 explained by among populations within groups, and 48.31% by within population
437 variation. These results agree with the population differentiation analysis (F_{ST} values;
438 Table 2).

439 A relationship between genetic differentiation and geographical distance
440 (Supplementary Table S7) was found among all sampled populations (Supplementary
441 Figure S2, r=0.735, P = 0.020), suggesting a strong isolation by distance effect at the
442 level of all populations. However, at a finer scale, when both sectors were analyzed
443 independently, no isolation by distance was observed.

444

445 *Recent gene flow and migration rates*

446 No migration between the eastern and western sectors could be detected by any of the
447 methods used. All individuals of the eastern sector were assigned by GENECLASS with
448 a probability of 90% or higher to their population of origin. In the western sector, 96%
449 of individuals originating from B1 and 88% of the individuals originating from B3 were
450 correctly assigned to their population of origin. Among the samples from B2, a total of
451 10.7% of individuals were assigned to B4 and 17.9% to B1, while the remaining 71% of
452 individuals were assigned to their population of origin. About 8.7% of the individuals
453 could not be assigned to any of the sampled populations. No first-generation migrants
454 were detected among populations from the eastern sector, and in the western sector only
455 one individual from B2 was detected to be migrant from B1 (P = 0.001). Although this
456 individual had a low probability of being a migrant from B1 (probability of migration of
457 0.038 according to analysis in STRUCTURE), it had an estimated posterior probability
458 of 0.231 to have a single parent from population B1. STRUCTURE results were similar
459 to GENECLASS assignments, with over 98% of the sampled individuals being assigned

460 to their population of origin. Estimates of recent gene flow using BIMr were consistent
461 among the five independent runs, suggesting that convergence of the Markov chain had
462 been reached. Recent migration rates showed no detectable recent gene flow between
463 populations within either the eastern or western sectors (Supplementary Table S8). The
464 overall outcome of the recent gene flow and migration rate analyses are in keeping with
465 the population structure detected above.

466

467 *Demographic history – effective population size (N_e)*

468 All three methods used to estimate the effective population sizes (N_e) of the seven
469 populations and of the two sectors (i.e. the two clusters identified by Structure) resulted,
470 in general, in low values, ranging from 7 to 342 (see Table 3). Estimation of the 95% CI
471 upper limit for populations A1 and A3 was problematic (estimated at infinity or
472 incongruence values) in the linkage disequilibrium method (LDNe). Despite slight
473 differences between methods, in general all estimators showed narrow CIs, thereby
474 supporting the accuracy of these estimates. Effective population sizes were particularly
475 low in population B3, with a 95% CI estimate of $N_e = 2 - 30$ regarding the three
476 methods used. Effective population sizes for the *C. asper* populations were similar or
477 higher than those of the *C. arnoldi* populations (Table 3).

478 Consistent with the previous results, MSVAR analysis also indicated relatively
479 small current N_e values for each of the six populations tested (B4 was not tested). For all
480 populations, the current effective population size seems to have been the outcome of a
481 reduction in N_e some time between 1,000 and 10,000 years ago, with the populations'
482 ancestral N_e being at maximum, one to two orders of magnitude larger than the current
483 one, e.g. N_0 A2 ~ 100, N_t A2 ~ 1,000 (Figure 3 and Supplementary Table S9). The ratio

484 of the ancestral N_e divided by the current N_e consistently result in values larger than 1
485 for all populations, providing further evidence for a decrease in N_e in the past of these
486 populations (Supplementary Figure S3). All MSVAR analyses showed convergent
487 results, as indicated by a Gelman & Rubin statistic being under 1.2, with the exception
488 of the clustered populations identified by STRUCTURE, where the MCMC did not
489 converge. Lastly, analyses performed in BOTTLENECK did not identify a significant
490 excess of heterozygosity in any of the sampled populations (nor in the sectors)
491 (Wilcoxon one tailed test for excess of heterozygosity p >0.05 for all tests), suggesting
492 that the bottleneck indicated by MSVAR probably did not cause a dramatic loss of
493 genetic diversity.

494

495 *Relatedness of individuals*

496 All populations presented a similar proportion of relatedness (Table 3), with most
497 individuals being highly unrelated to each other (80%). The only exception was
498 population B3, which had a lower percentage of unrelated specimens (68%). Full
499 sibling and parent-offspring relations in B3 were 12 and 11%, respectively, while the
500 other populations showed much lower percentages, none exceeding 4%. The estimated
501 Queller & Goodnight (1989) index of relatedness, calculated between individuals in
502 each population separately, indicated random mating among individuals within each
503 population, i.e. panmixia within populations (A1, r_{qg} = -0.045; A2, r_{qg} = -0.038; A3, r_{qg}
504 = -0.038; B1, r_{qg} = -0.042; B2, r_{qg} = -0.037; B3, r_{qg} = -0.067; B4, r_{qg} = -0.333).
505 Conversely, at the sector level (i.e. when testing whether there is random mating
506 between populations within a sector), values ranged from 0.150 to 0.206 and from 0.019
507 to 0.231 within the eastern western sectors respectively, with the only exception being

population B3, which showed an average pairwise relatedness (r_{qg}) of 0.745 (upper and lower CI estimates at 95% of 0.759 and 0.730, respectively). Most populations demonstrated significantly higher relatedness than could be expected if each sector represented a panmictic population. Thus, consistent with our results of the gene flow and migration rate analysis, this suggests random mating among individuals from distinct populations within sectors does not occur (Supplementary Figure S4). These results are concordant with the lack of migration among populations indicated by other analyses. Similar values of relatedness were detected for the reference *C. asper* populations (Table 3) and r_{qg} (Ibón de Perramó, r_{qg} = -0.031; Barranco de Valdragás, r_{qg} = -0.026; Ibón de Acherito, r_{qg} = -0.046; Bassies, r_{qg} = -0.005).

Discussion

Habitat fragmentation is typically expected to lead to a decrease in genetic diversity due to stochastic processes (e.g. genetic drift), which have a stronger effect in smaller populations (Leimu *et al.* 2006). Therefore, species restricted to small geographic areas may experience a high risk of extinction if populations become fragmented and isolated from each other. However, there is also some evidence to suggest that habitat fragmentation can give rise to neutral or even positive effects (Fahrig 2003; Templeton *et al*. 1990). Here we show that extreme subdivision in an amphibian species (*Calotriton arnoldi*) has not negatively affected certain genetic parameters that are supposed to be important indicators for fitness, such as genetic diversity and inbreeding coefficients, when compared to non-fragmented populations of its sister species (*C. asper*).

532 *Phylogenetic divergence*

533 The estimated divergence between the two species of *Calotriton* confirms previous
534 dating analyses (Carranza & Amat 2005), and indicates that these species split
535 approximately 1.5 Mya, during the Pleistocene epoch. Speciation within *Calotriton* may
536 have been initiated by a geographical barrier, or could have resulted from climatic
537 fluctuations during the Pleistocene. Following the challenging climatic conditions of the
538 last glacial maximum, the high dispersal capabilities of the Pyrenean brook newt helps
539 to explain its rapid dispersion through the Pyrenean axial chain and the Prepyrenees;
540 this allowed the connection of populations and subsequent genetic homogenization as a
541 consequence of gene flow (Valbuena-Ureña *et al*. 2013). In contrast to *C. asper*, a
542 juvenile dispersal phase is absent in *C. arnoldi*, therefore hindering its capacity for
543 colonization. This species probably found refuge in the Montseny massif, being unable
544 to colonize areas beyond the Montseny mountain. The differentiation into two sectors
545 seems to be relatively ancient (~180,000 years ago), coinciding with the Riss glaciation
546 (300,000 – 130,000 ya). This glaciation is characterized by a significant temperature
547 drop and dry climate, which may have decreased the water flow of the Tordera River,
548 causing the extinction of intermediate populations between the current populated sites.
549 Such a scenario is further corroborated by differences in morphology, as well as
550 mitochondrial and nuclear coding genes between the sectors (Valbuena-Ureña *et al.*
551 2013), suggesting that the fragmentation into subpopulations is not a recent event driven
552 by anthropogenic activities, but rather by natural processes. As our results indicate
553 (Figure 3), the effective population sizes of *C. arnoldi* populations have remained low
554 since the species split.

555 Neutral genetic diversity is shaped by the balance of evolutionary forces
556 (mutation, genetic drift and migration) over contemporary and historical time-scales

557 (Dalongeville *et al*. 2016). Although genetic diversity greatly depends on the age of the
558 population concerned, the *Calotriton* species have diverged relatively recently and both
559 have experienced similar historical climatic events (Valbuena-Ureña *et al*. 2013);
560 therefore, the comparison between them is appropriate (Hendrix *et al.* 2010).
561

562 *Patterns of genetic diversity*

563 Due to lower vagility, loss of genetic diversity in amphibians is likely to be greater than
564 in many other taxa, and is highly correlated with declines in population fitness and the
565 diminishment of their adaptive potential (Allentoft & O'Brien 2010). Overall, it appears
566 that across its small and restricted distribution range, moderate levels of genetic
567 diversity and high genetic differentiation among sites characterize the Montseny brook
568 newt. The comparison of genetic variation between this species and its closely related
569 and ecologically similar sister species *C. asper* indicates that in general, *C. arnoldi*
570 harbors similar levels of genetic diversity despite its far smaller distribution range. The
571 differences detected in the western sector are mostly due to population B3. We can state
572 that population B3 differs from all other populations of the same species, not only from
573 *C. asper* populations. Therefore, we believe these data do not support a general pattern
574 in which the western sector significantly differs from the four randomly selected *C.*
575 *asper* populations. It seems that population B3 is an example of a fragile population in
576 terms of low genetic diversity and low effectives rather than a situation in which the
577 entire sector suffers the effects of habitat fragmentation. Moreover, neither species show
578 signs of inbreeding. *C. asper* shows similar or slightly higher values of N_e than *C.*
579 *arnoldi*. While *C. asper* has a juvenile dispersal phase that may reduce risk of
580 inbreeding, *C. arnoldi* is exclusively aquatic with no dispersal phase, and may therefore
581 have developed other mechanisms to counteract the genetic consequences of small

582 populations sizes. It is surprising that populations of *C. arnoldi* display similar levels of
583 genetic variation to *C. asper* despite their differences in range size, despite *C. arnoldi*
584 effective population size, and the evidence of a past bottleneck. However, when
585 comparing the expected heterozygosity of *C. arnoldi* to that of other salamanders and
586 temperate amphibians, *C. arnoldi* is within the typical range (0.4 – 0.6; Chan &
587 Zamudio 2009 and references therein).

588 Our results clearly show that *C. arnoldi* populations are highly structured over
589 short geographic distances, and the species is differentiated into an eastern and a
590 western sector (Figure 2). Interestingly, the eastern sector presents higher levels of
591 genetic variability than the western sector both in terms of microsatellite loci and
592 nuclear and mitochondrial DNA sequences (Valbuena-Ureña *et al.* 2013). The most
593 likely explanation for this pattern is the larger effective population sizes of the eastern
594 populations in comparison to the western ones.

595 That the two sectors are highly genetically differentiated, with no gene flow
596 between them, is indicated by multiple lines of evidence, including: a large number of
597 private alleles in each sector (75 and 38 in the eastern and western sectors,
598 respectively); significantly different patterns of genetic variation between sectors (e.g.
599 AMOVA, allelic richness and the number of fixed alleles in each sector); outcome of
600 the PCA analysis; high F_{ST} values; unambiguous genetic assignment of individuals to
601 their population of origin; and observed isolation by distance effect. Since *C. arnoldi* is
602 exclusively aquatic, dispersal can only occur along watercourses, therefore reducing
603 dispersal capabilities with respect to similar species capable of terrestrial dispersal. This
604 is reflected in the levels of genetic differentiation observed, which are notably higher
605 than values typically found for amphibians that use both aquatic and terrestrial habitats
606 (Spear *et al.* 2005). The sectors of *C. arnoldi* are effectively isolated by a 37 km long

607 watercourse, whereas distance by land is only 6 km. The watercourse between the two
608 sectors passes through long stretches of river which includes a low altitude (<600 m)
609 section with high water temperatures and potential predators; it therefore constitutes an
610 adverse environment for these aquatic newts and thus presents a strong migration
611 barrier. Accordingly, we can assume that in this system, natural fragmentation has
612 played a strong impact on observed and associated microevolutionary processes (see
613 Templeton *et al.* 1990).

614 Although the strong population subdivision is clearly detected between sectors,
615 the low dispersal capability of this species is also detected among populations within
616 sectors. The significant F_{ST} values indicate that dispersal between populations is low, as
617 confirmed by the differentiation of populations/clusters A3 and B3 from the other
618 populations within their respective sectors. These results were consistent with the
619 outcome of PCA analysis and migration tests. Moreover, at a sector level, most
620 populations showed significantly higher degrees of relatedness (r_{qg}) than expected if
621 sectors were in panmixia. This pattern is expected when migration among populations is
622 not sufficiently high to counteract the relatedness resulting from nonrandom mating
623 among populations. This notable sector structuring could suggest high levels of
624 relatedness and inbreeding of individuals within populations. However, this is not
625 found, as non-relatedness values within populations remain high, and random mating
626 within populations seems to occur (see discussion below).

627 Our results indicate that the overall genetic diversity of *C. arnoldi* has been
628 maintained at relatively high levels across its small and fragmented distribution range.
629 This species comprises of highly genetically differentiated populations which display
630 moderate levels of genetic diversity. Therefore, both intrapopulation genetic diversity
631 levels and the strong differentiation among them allow this species to retain enough

632 genetic variation to persist despite the vulnerability inherent in its small distribution
633 range.

634

635 *The impact of natural fragmentation on C. arnoldi*

636 It is broadly accepted that habitat fragmentation (either naturally occurring or human
637 driven) will result in the subdivision of populations and, if migration of individuals is
638 not possible, subpopulations will start to diverge genetically (Frankham *et al.* 2010;
639 Templeton *et al.* 1990). However, Templeton *et al.* (1990) suggested that despite the
640 negative effects deriving from fragmentation, genetic variation is not completely lost,
641 but often presents as fixed differences between local populations. Although this aspect
642 is relevant for species conservation, it is little considered at present, and pertinent case
643 studies are lacking. In our view, the surprising results obtained herein, involving an
644 endangered species affected by natural habitat fragmentation, provide an excellent study
645 system to promote discussion on this overlooked aspect.

646 Both the census and effective population sizes in *C. arnoldi* rank it as a critically
647 endangered species; current N_e values for all *C. arnoldi* populations are critically low
648 (<50) and are consistent with the small census size (Carranza & Martínez-Solano 2009).
649 The divergence time estimated between *C. asper* and *C. arnoldi*, and between the two
650 *C. arnoldi* sectors, indicates that these splits were not recent events (over 1 Mya the
651 former and over 100 Kya for the latter). Moreover, the N_e values estimated for *C.*
652 *arnoldi* indicate a small population size throughout its comparable short evolutionary
653 history of roughly 1.76 Mya. These facts support the hypothesis that after the
654 divergence of the two species, *C. asper* went through a rapid expansion phase, while *C.*
655 *arnoldi* remained geographically restricted. The current distribution range of *C. asper*

populations cover an area of roughly 20,000 km^2, while populations of *C. arnoldi* are restricted to an area of only 8 km^2; such differences are expected to be reflected in genetic parameters, and yet they are not.

In general, different behavioral strategies can be assumed for animals to avoid inbreeding. The most easy and obvious strategy would be postnatal dispersal of individuals to reduce the probability of inbreeding, the second would be mating preferences for non-related individuals (Blouin & Bloiun 1988). Based on the high degree of genetic differentiation and the lack of migration between *C. arnoldi* subpopulations between the two sectors, we can basically exclude postnatal dispersal as a mechanism to avoid inbreeding. It is therefore likely that special mating preferences exist in *C. arnoldi* to minimize the effects of potential inbreeding. As we have not observed an excess of heterozygosity for analysed microsatellite loci across sectors, we can further conclude that females – assuming that they are the choosing sex – might not only prefer to mate with unrelated males but also with related ones. Indeed, more recent empirical studies – in contrast to early ones – indicate that animals sometimes show no avoidance or even prefer to mate with relatives (see Szuklin *et al*. 2013). In crickets, for example, Tregenza & Wedell (2002) could show that females mating multiply with different males avoid low egg viability, which occurs when solely mating with non-related or only with related males, if they mate with both unrelated and related males. Sperm storage in special cloacal glands of the female (called spermathecae) in combination with multiple paternity is widespread and well documented for salamander and newt species of the suborder Salamandroidea, to which also *Calotriton* newts belong (Kühnel *et al.* 2010; Caspers *et al*. 2014). Although we are lacking direct evidence, it is very likely that females of *C. arnoldi* mate multiply with different males, resulting in multiple paternities. Assuming similar mating patterns as described above

for crickets, *C. arnoldi* newts could avoid the negative consequences of inbreeding without displaying an excess of heterozygosity. Of course, at the moment it is completely unclear and needs further investigation by which behavioral mechanisms these newts can cope with small sizes of fragmented populations.

Overall, our results suggest that in terms of maintaining genetic diversity, small effective population sizes do not necessarily pose a problem, as there may be other reproductive or behavioral mechanisms that can counteract the effects of genetic drift (Allentoft & O'Brien 2010). In *C. arnoldi,* such mechanisms are likely to have prevented a substantial loss of alleles through the bottleneck experienced during the Holocene. Evidence suggests that life history strategies can explain a considerable proportion of the variation in genetic diversity, as polymorphism levels are influenced by species biology (Dalongeville *et al*. 2016; Fouquet *et al*. 2015; Paz *et al*. 2015; Romiguier *et al*. 2014). Ecological factors affecting genetic diversity may include migration capability, morphological or physiological adaptations, and reproductive strategy, amongst others.

Our results indicate that the overall genetic diversity of *C. arnoldi* has been maintained at a relatively high level despite its small and fragmented distribution range. Therefore, species fragmentation should not be regarded in this case as primarily detrimental. Populations of *C. arnoldi* do not show the low levels of intrapopulation genetic diversity or signs of inbreeding that are typical byproducts of habitat fragmentation. However, data regarding the potential effect of the fragmentation on a species potential to adapt to environmental changes, which again may be influenced by the life-history strategies, are currently lacking (Dalongeville *et al*. 2016; Romiguier *et al*. 2014). Further studies are needed to understand the relationship between genetic diversity, adaptive potential, and life-history traits in this species.

706 Species characterized by independent and isolated populations may avoid
707 species-level extinction, since local (population-level) extinctions, resulting from local
708 demographic stochasticity or small-scale environmental catastrophes are unlikely to be
709 simultaneously experienced by all populations. Furthermore, in terms of infectious
710 diseases (e.g. parasite infections or bacterial pathogens such as those causing the "Red-
711 leg" syndrome; Allentoft & O'Brien 2010; Daszak *et al*. 2003), populations that are
712 completely isolated might survive an outbreak since there is little or no exchange of
713 individuals between single populations. Therefore, the persistence of some populations
714 facilitates the survival of the species, and recolonization may occur over time, thus
715 reversing extirpations.

716

717 *Implications for conservation*

718 Impacts of habitat fragmentation must be measured independently from effects of
719 habitat loss or degradation. The effects of habitat loss may outweigh the effects of
720 habitat fragmentation, and can have important implications for conservation. Habitat
721 loss is widely recognized to have strong and consistently negative effects on
722 biodiversity, reducing species richness, population abundance and distribution, and
723 genetic diversity (Fahrig 2003 and references therein).

724 In conservation biology, a N_e of 500 has been suggested as a minimum value for
725 the long-term survival of a species, whereas N_e values below 50 in isolated populations
726 are of major concern (Frankham *et al*. 2014), since these populations have an increased
727 probability of extinction resulting from genetic effects like inbreeding (Allendorf &
728 Luikart 2007) and stochastic environmental processes. Inbreeding is exacerbated by
729 small N_e values. However, it is possible that populations with low N_e may survive over

730 long periods of time as they can successfully and rapidly purge detrimental allelic
731 variants, such a scenario has been proposed for other species (e.g. Orozco-terWengel *et*
732 *al*. 2015). However, the current low effective population sizes of *C. arnoldi* mean that
733 habitat loss or degradation could rapidly drive these small populations to extinction.
734 Stochastic factors can cause a disproportionately high mortality rate when species have
735 very small distribution ranges. Moreover, the effects of habitat loss may be greater
736 when the habitat is highly and rapidly fragmented. This implies that a key question
737 concerning the conservation of a species is "how much habitat is enough?". The
738 conservation of a vulnerable or endangered species requires estimating the minimum
739 habitat required for persistence of the given species. In addition, many species require
740 more than one kind of habitat within a life cycle. Therefore, landscape patterns that
741 maintain the required habitat proportions should be conserved (Fahrig 2003).

742 Studies which enhance understanding of genetic population structure and the
743 gene flow between them contribute valuable information to management and
744 conservation programs. The definition of appropriate conservation units are crucial for
745 maintaining the distinct evolutionary lineages and the species' evolutionary potential
746 (Frankham *et al.* 2010). In *C. arnoldi,* the evolutionary potential is not only manifested
747 within the species as a whole, but also within each sector. Conservation strategies
748 should be adopted to ensure that the evolutionary potential and the genetic diversity
749 within the distinct groups is not lost. Therefore, such strategies should focus on habitat
750 preservation and restoration of each sector, with the aim of maintaining the strong
751 population structure highlighted by this study.
752

753 **Acknowledgements**

We are grateful to all members of the CRFS Torreferrussa, and especially to M. Alonso, F. Carbonell, E. Obon and R. Larios. We also thank the DAAM department of the Generalitat de Catalunya, the staff of Parc Natural del Montseny of the Diputació de Barcelona, and F. Amat. We are very grateful to Amy MacLeod (EditingZoo) for the English editing. This research was supported by Miloca and Zoo de Barcelona (PRIC-2011). S.C. is supported by a grant CGL2012-36970 from the Ministerio de Economía y Competitividad, Spain (co-funded by FEDER). We thank Ralf Hendrix for performing the primary microsatellite loci analysis in the laboratory.

Conflict of interest

The authors declare no conflict of interests.

Data archiving

Data deposited in the Dryad repository: xxxxx

References

Akaike H (1973) Information theory and an extension of the maximum likelihood principle. In: *Second International Symposium on Information Theory* (eds. Petrov BN, Csaki F), pp. 267-281. Akademiai Kiado, Budapest, Hungary.

Allendorf FW, Luikart G (2007) *Conservation and the Genetics of Populations* Blackwell, Oxford.

Allentoft M, O'Brien J (2010) Global amphibian declines, loss of genetic diversity and fitness: a review. *Diversity* **2**, 47-71.

777 Amat F, Carranza S, Valbuena-Ureña E, Carbonell F (2014) Saving the Montseny brook
778 newt (*Calotriton arnoldi*) from extinction: an assessment of eight years of
779 research and conservation. *Froglog* **22**, 55-57.
780 Apodaca J, Rissler L, Godwin J (2012) Population structure and gene flow in a heavily
781 disturbed habitat: implications for the management of the imperilled Red Hills
782 salamander (*Phaeognathus hubrichti*). *Conservation Genetics* **13**, 913-923.
783 Arèvalo E, Davis SK, Sites JW (1994) Mitochondrial DNA sequence divergence and
784 phylogenetic relationships among eight chromosome races of the *Sceloporus*
785 *grammicus* complex (Phrynosomatidae) in Central Mexico. *Systematic Biology*
786 **43**, 387-418.
787 Belkhir K, Chikhi L, Raufaste N, Bonhomme F (2004) GENETIX 4.05, logiciel sous
788 Windows TM pour la génétique des populations. Laboratoire Génome,
789 Populations, Interactions, CNRS UMR 5000: Université de Montpellier II,
790 Montpellier (France).
791 Blank L, Sinai I, Bar-David S, Peleg N, Segev O, Sadeh A, Kopelman NM *et al*. (2013)
792 Genetic population structure of the endangered fire salamander (*Salamandra*
793 *infraimmaculata*) at the southernmost extreme of its distribution. *Animal*
794 *Conservation* **16**, 412-421.
795 Blouin SF, Blouin M (1988) Inbreeding avoidance behaviours. *Trends in ecology &*
796 *evolution* **3**, 230-233.
797 Blouin M, Phillipsen I, Monsen K (2010) Population structure and conservation
798 genetics of the Oregon spotted frog, *Rana pretiosa*. *Conservation Genetics* **11**,
799 2179-2194.
800 Brooks SP, Gelman A (1998) General methods for monitoring convergence of iterative
801 simulations. *Journal of Computational and Graphical Statistics* **7**, 434-455.

802 Bulut Z, McCormick C, Gopurenko D, Williams R, Bos D, DeWoody JA (2009)
803 Microsatellite mutation rates in the eastern tiger salamander (*Ambystoma*
804 *tigrinum tigrinum*) differ 10-fold across loci. *Genetica* **136**, 501-504.
805 Carranza S, Amat F (2005) Taxonomy, biogeography and evolution of *Euproctus*
806 (Amphibia: Salamandridae), with the resurrection of the genus *Calotriton* and
807 the description of a new endemic species from the Iberian Peninsula. *Zoological*
808 *Journal of the Linnean Society* **145**, 555-582.
809 Carranza S, Arnold EN, Mateo JA, López-Jurado LF (2000) Long-distance colonization
810 and radiation in gekkonid lizards, *Tarentola* (Reptilia: Gekkonidae), revealed by
811 mitochondrial DNA sequences. *Proceedings of the Royal Society of London.*
812 *Series B: Biological Sciences* **267**, 637-649.
813 Carranza S, Martínez-Solano I (2009) *Calotriton arnoldi.* IUCN Red List of Threatened
814 Species. Version 2012.1
815 Caspers BA, Krause ET, Hendrix R, Kopp M, Rupp O, Rosentreter K *et al*. (2014) The
816 more the better – polyandry and genetic similarity are positively linked to
817 reproductive success in a natural population of terrestrial salamanders
818 (*Salamandra salamandra*). *Molecular Ecology* **23**, 239-250.
819 Chan LM, Zamudio KR (2009) Population differentiation of temperate amphibians in
820 unpredictable environments. *Molecular Ecology* **18**, 3185-3200.
821 Dalongeville A, Andrello M, Mouillot D, Albouy C, Manel S (2016) Ecological traits
822 shape genetic diversity patterns across the Mediterranean Sea: a quantitative
823 review on fishes. *Journal of Biogeography* **43**, 845-857.
824 Darriba D, Taboada GL, Doallo R, Posada D (2012) jModelTest 2: more models, new
825 heuristics and parallel computing. *Nature Methods* **9**, 772-772.

826 Daszak P, Cunningham AA, Hyatt AD (2003) Infectious disease and amphibian
827 population declines. *Diversity and Distributions* **9**, 141-150.
828 Drechsler A, Geller D, Freund K, Schmeller DS, Künzel S, Rupp O *et al*. (2013) What
829 remains from a 454 run: estimation of success rates of microsatellite loci
830 development in selected newt species (*Calotriton asper*, *Lissotriton helveticus*,
831 and *Triturus cristatus*) and comparison with Illumina-based approaches. *Ecology*
832 *and Evolution* **3**, 3947-3957.
833 Drummond A, Rambaut A (2007) BEAST: Bayesian evolutionary analysis by sampling
834 trees. *BMC Evolutionary Biology* **7**, 214.
835 Earl D, vonHoldt B (2012) STRUCTURE HARVESTER: a website and program for
836 visualizing STRUCTURE output and implementing the Evanno method.
837 *Conservation Genetics Resources* **4**, 359-361.
838 Evanno G, Regnaut S, Goudet J (2005) Detecting the number of clusters of individuals
839 using the software structure: a simulation study. *Molecular Ecology* **14**, 2611-
840 2620.
841 Excoffier L, Lischer HEL (2010) Arlequin suite ver 3.5: a new series of programs to
842 perform population genetics analyses under Linux and Windows. *Molecular*
843 *Ecology Resources* **10**, 564-567.
844 Fahrig L (2003) Effects of habitat fragmentation on biodiversity. *Annual Review of*
845 *Ecology, Evolution, and Systematics* **34**, 487-515.
846 Faubet P, Gaggiotti OE (2008) A new bayesian method to identify the environmental
847 factors that influence recent migration. *Genetics* **178**, 1491-1504.
848 Fouquet A, Courtois EA, Baudain D, Lima JD, Souza SM, Noonan BP *et al*. (2015) The
849 trans-riverine genetic structure of 28 Amazonian frog species is dependent on
850 life history. *Journal of Tropical Ecology* **31**, 361-373.

851 Frankham R, Ballou JD, Briscoe DA (2010) *Introduction to Conservation Genetics*, 2nd
852 edn. Cambridge University Press, Cambridge.
853 Frankham R, Bradshaw CJ, Brook BW (2014) Genetics in conservation management:
854 revised recommendations for the 50/500 rules, Red List criteria and population
855 viability analyses. Biological Conservation **170**, 56-63.
856 Gerlach G, Jueterbock A, Kraemer P, Deppermann J, Harmand P (2010) Calculations of
857 population differentiation based on GST and D: forget GST but not all of
858 statistics! *Molecular Ecology* **19**, 3845-3852.
859 Goudet J (1995) FSTAT (Version 1.2): A computer program to calculate F-statistics.
860 *Journal of Heredity* **86**, 485-486.
861 Guo SW, Thompson EA (1992) Performing the exact test of Hardy-Weinberg
862 proportion for multiple alleles. *Biometrics* **48**, 361-372.
863 Hauswaldt JS, Angelini C, Gehara M, Benavides E, Polok A, Steinfartz S (2014) From
864 species divergence to population structure: A multimarker approach on the most
865 basal lineage of Salamandridae, the spectacled salamanders (genus
866 *Salamandrina*) from Italy. *Molecular Phylogenetics and Evolution* **70**, 1-12.
867 Hendrix R, Susanne Hauswaldt J, Veith M, Steinfartz S (2010) Strong correlation
868 between cross-amplification success and genetic distance across all members of
869 'True Salamanders' (Amphibia: Salamandridae) revealed by Salamandra
870 salamandra-specific microsatellite loci. *Molecular Ecology Resources* **10**, 1038-
871 1047.
872 Hill WG (1981) Estimation of effective population size from data on linkage
873 disequilibrium. *Genetics Research* **38**, 209-216.
874 Huelsenbeck JP, Larget B, Miller RE, Ronquist F (2002) Potential applications and
875 pitfalls of bayesian inference of phylogeny. *Systematic Biology* **51**, 673-688.

876 Jakobsson M, Rosenberg NA (2007) CLUMPP: a cluster matching and permutation
877 program for dealing with label switching and multimodality in analysis of
878 population structure. *Bioinformatics* **23**, 1801-1806.
879 Jones OR, Wang J (2010) COLONY: a program for parentage and sibship inference
880 from multilocus genotype data. *Molecular Ecology Resources* **10**, 551-555.
881 Jost L (2008) GST and its relatives do not measure differentiation. *Molecular Ecology*
882 **17**, 4015-4026.
883 Kalinowski ST (2005) hp-rare 1.0: a computer program for performing rarefaction on
884 measures of allelic richness. *Molecular Ecology Notes* **5**, 187-189.
885 Kalinowski ST, Wagner AP, Taper ML (2006) ML-RELATE: a computer program for
886 maximum likelihood estimation of relatedness and relationship. *Molecular*
887 *Ecology Notes* **6**, 576-579.
888 Katoh K, Standley DM (2013) MAFFT Multiple sequence alignment software version
889 7: improvements in performance and usability. *Molecular Biology and Evolution*
890 **30**, 772-780.
891 Kühnel S, Reinhard S, Kupfer A (2010) Evolutionary reproductive morphology of
892 amphibians: an overview. *Bonn Zoological Bulletin* **57**, 119-126.
893 Leimu R, Mutikainen PIA, Koricheva J, Fischer M (2006) How general are positive
894 relationships between plant population size, fitness and genetic variation?
895 *Journal of Ecology* **94**, 942-952.
896 Lewis PO, Zaykin D (2000) Genetic data analysis: computer program for the analysis of
897 allelic data, version 1.0. (d15), University of Connecticut, Storrs, Connecticut,
898 USA.

MacLeod A, Rodríguez A, Vences M, Orozco-terWengel P, García C, Trillmich F *et al*. (2015) Hybridization masks speciation in the evolutionary history of the Galápagos marine iguana. *Proceedings of the Royal Society B* **282**, 20150425.

Mantel N (1967) The detection of disease clustering and a generalized regression approach. *Cancer Research* **27**, 209-220.

Martínez-Solano I, Teixeira J, Buckley D, García-París M (2006) Mitochondrial DNA phylogeography of Lissotriton boscai (Caudata, Salamandridae): evidence for old, multiple refugia in an Iberian endemic. *Molecular Ecology* **15**, 3375-3388.

Milá B, Carranza S, Guillaume O, Clobert J (2010) Marked genetic structuring and extreme dispersal limitation in the Pyrenean brook newt *Calotriton asper* (Amphibia: Salamandridae) revealed by genome-wide AFLP but not mtDNA. *Molecular Ecology* **19**, 108-120.

Monsen KJ, Blouin MS (2004) Extreme isolation by distance in a montane frog *Rana cascadae*. *Conservation Genetics* **5**, 827-835.

Nosil P, Funk DJ, Ortiz-Barrientos D (2009) Divergent selection and heterogeneous genomic divergence. *Molecular Ecology* **18**, 375-402

Orozco-terWengel P, Barbato M, Nicolazzi E, Biscarini F, Milanesi M, Davies W, *et al*. (2015) Revisiting demographic processes in cattle with genome-wide population genetic analysis. *Frontiers in genetics* **6**,191.

Paetkau D, Slade R, Burden M, Estoup A (2004) Genetic assignment methods for the direct, real-time estimation of migration rate: a simulation-based exploration of accuracy and power. *Molecular Ecology* **13**, 55-65.

Paz A, Ibáñez R, Lips KR, Crawford AJ (2015) Testing the role of ecology and life history in structuring genetic variation across a landscape: a trait-based phylogeographic approach. *Molecular Ecology* **24**, 3723-3737.

924 Peakall R, Smouse PE (2006) GENALEX 6: genetic analysis in Excel. Population
925 genetic software for teaching and research. *Molecular Ecology Notes* **6**, 288-
926 295.
927 Piry S, Luikart G, Cornuet JM (1999) BOTTLENECK: A computer program for
928 detecting recent reductions in the effective population size using allele frequency
929 data. *Journal of Heredity* **90(4)**, 502-503.
930 Piry S, Alapetite A, Cornuet J-M, Paetkau D, Baudouin L, Estoup A (2004)
931 GENECLASS2: a software for genetic assignment and first-generation migrant
932 detection. *Journal of Heredity* **95**, 536-539.
933 Plummer M, Best N, Cowles K, Vines K (2006) Coda: convergence diagnosis and
934 output analysis for MCMC. *R news* **6**, 7-11.
935 Pritchard JK, Stephens M, Donnelly P (2000) Inference of population structure using
936 multilocus genotype data. *Genetics* **155**, 945-959.
937 Queller DC, Goodnight KF (1989) Estimating relatedness using genetic markers.
938 *Evolution* **43**, 258-275.
939 Rambaut A, Drummond A (2007) *Tracer v1.5 <http://beast.bio.ed.ac.uk/Tracer>*.
940 Recuero E, Canestrelli D, Vörös J, Szabó K, Poyarkov NA, Arntzen JW *et al*. (2012)
941 Multilocus species tree analyses resolve the radiation of the widespread *Bufo*
942 *bufo* species group (Anura, Bufonidae). *Molecular Phylogenetics and Evolution*
943 **62**, 71-86.
944 Romiguier J, Gayral P, Ballenghien M, Bernard A, Cahais V, Chenuil A *et al*. (2014)
945 Comparative population genomics in animals uncovers the determinants of
946 genetic diversity. *Nature* **515**, 261-263.
947 Rosenberg NA (2004) DISTRUCT: a program for the graphical display of population
948 structure. *Molecular Ecology Notes* **4**, 137-138.

949 Rousset F (1997) Genetic differentiation and estimation of gene flow from F-statistics
950 under isolation by distance. *Genetics* **145**, 1219-1228.
951 Rousset F (2008) Genepop'007: a complete re-implementation of the genepop software
952 for Windows and Linux. *Molecular Ecology Resources* **8**, 103-106.
953 Savage WK, Fremier AK, Bradley Shaffer H (2010) Landscape genetics of alpine Sierra
954 Nevada salamanders reveal extreme population subdivision in space and time.
955 *Molecular Ecology* **19**, 3301-3314.
956 Slatkin M (1994) Gene flow and population structure. In: *Ecological genetics* (ed. LA
957 R), pp. 3-17. Princeton University Press, Princeton, New Jersey.
958 Šmíd J, Carranza S, Kratochvíl L, Gvoždík V, Nasher AK, Moravec J (2013) Out of
959 Arabia: a complex biogeographic history of multiple vicariance and dispersal
960 events in the gecko genus *Hemidactylus* (Reptilia: Gekkonidae). *PLoS ONE* **8**,
961 e64018.
962 Smith MA, Green DM (2005) Dispersal and the metapopulation paradigm in amphibian
963 ecology and conservation: are all amphibian populations metapopulations?
964 *Ecography* **28**, 110-128.
965 Spear SF, Peterson CR, Matocq MD, Storfer A (2005) Landscape genetics of the
966 blotched tiger salamander (*Ambystoma tigrinum melanostictum*). *Molecular*
967 *Ecology* **14**, 2553-2564.
968 Steinfartz S, Weitere M, Tautz D (2007) Tracing the first step to speciation: ecological
969 and genetic differentiation of a salamander population in a small forest.
970 *Molecular Ecology* **16**, 4550-4561.
971 Storfer A, Mech S, Reudink M, Lew K (2013) Inbreeding and strong population
972 subdivision in an endangered salamander. *Conservation Genetics*, 1-15.

973 Storz JF, Beaumont MA (2002) Testing for genetic evidence of population expansion
974 and contraction: an empirical analysis of microsatellite DNA variation using a
975 hierarchical bayesian model. *Evolution* **56**, 154-166.

976 Sunny A, Monroy-Vilchis O, Fajardo V, Aguilera-Reyes U (2014) Genetic diversity
977 and structure of an endemic and critically endangered stream river salamander
978 (Caudata: *Ambystoma leorae*) in Mexico. *Conservation Genetics* **15**, 49-59.

979 Szulkin M, Stopher KV, Pemberton JM, Reid JM (2013) Inbreeding avoidance,
980 tolerance, or preference in animals? *Trends in ecology & evolution* **28**, 205-211..

981 Tallmon DA, Koyuk A, Luikart G, Beaumont MA (2008) COMPUTER PROGRAMS:
982 onesamp: a program to estimate effective population size using approximate
983 Bayesian computation. *Molecular Ecology Resources* **8**, 299-301.

984 Templeton AR, Shaw K, Routman E, Davis SK (1990) The genetic consequences of
985 habitat fragmentation. *Annals of the Missouri Botanical Garden* **77**, 13-27.

986 Tregenza T, Wedell N (2002) Polyandrous females avoid costs of inbreeding. *Nature*
987 **415**, 71–73.

988 Valbuena-Ureña E, Amat F, Carranza S (2013) Integrative phylogeography of
989 *Calotriton* newts (Amphibia, Salamandridae), with special remarks on the
990 conservation of the endangered Montseny brook newt (*Calotriton arnoldi*).
991 *PLoS ONE* **8**, e62542.

992 Valbuena-Ureña E, Steinfartz S, Carranza S (2014) Characterization of microsatellite
993 loci markers for the critically endangered Montseny brook newt (*Calotriton*
994 *arnoldi*). *Conservation Genetics Resources* **6**, 263-265.

995 Van Oosterhout C, Hutchinson WF, Wills DPM, Shipley P (2004) Micro-checker:
996 software for identifying and correcting genotyping errors in microsatellite data.
997 *Molecular Ecology Notes* **4**, 535-538.
998 Veith M, Kosuch J, Vences M (2003) Climatic oscillations triggered post-Messinian
999 speciation of Western Palearctic brown frogs (Amphibia, Ranidae). *Molecular*
1000 *Phylogenetics and Evolution* **26**, 310-327.
1001 Velo-Antón G, Parra JL, Parra-Olea G, Zamudio KR (2013) Tracking climate change in
1002 a dispersal-limited species: reduced spatial and genetic connectivity in a
1003 montane salamander. *Molecular Ecology* **22**, 3261-3278.
1004 Waples RS, Do C (2008) LDNE: a program for estimating effective population size
1005 from data on linkage disequilibrium. *Molecular Ecology Resources* **8**, 753-756.
1006 Weir BS, Cockerham CC (1984) Estimating F-statistics for the analysis of population
1007 structure. *Evolution* **38**, 1358-1370.
1008

Table 1. Estimates of genetic parameters for each *Calotriton arnoldi* population and cluster defined by STRUCTURE analysis, and for the four *C. asper* populations. Values represent averages across 24 loci. N, sample size; A, number of alleles per locus; Ar, allelic richness; PA, number of private alleles; PAAr, allelic richness of private alleles; H_O, observed heterozygosity; H_E, expected heterozygosity; F_{IS}, inbreeding coefficient. Values in bold indicate statistical significance after Bonferroni correction.

Table 2. Genetic differentiation among populations. Pairwise F_{ST}, below the diagonal; D estimator values above the diagonal. All *P* values were significant ($P < 0.001$).

Table 3. Estimates of effective population size *(N_e)* for each population and cluster of *Calotriton arnoldi* and for the four *C. asper* populations, calculated with three programs: LDNe, ONeSAMP and COLONY; estimations of the upper and lower 95% CI estimates for each method are indicated. Relationship indicates the percentage of individual relatedness within each population and cluster.

Table S1. Specimens of *Calotriton* included in the molecular analyses. For all 24 specimens newly sequenced in the present study, we provide their taxonomic identification, sample code and GenBank accession numbers. Population and corresponding locality are shown in the map from Figure 1A.

Table S2. Characterization of the full set of 24 applied microsatellite loci for *Calotriton arnoldi*. Loci are grouped by multiplex combinations used for amplification. Locus name, primer sequence, direction (F is forward, R is reverse), annealing temperature of the primer for PCRs, microsatellite motif, amplified fragment size range, number of alleles, labeling dye, and references are provided.

Table S3. Prior distributions used for the MsVar analysis. N_0= current effective population size, N_t= ancestral effective population size, t= time of the change from N_0 to

N_t, and m= mutation rate. M is the mean of a parameter and V its variance. Means of means and variances of means for the hyperpriors were the same as for the mean and variance of each parameter in the priors, and the hyperprior's mean of variances and variance of variances were 0 and 0.5, respectively.

Table S4. Estimates of genetic parameters for each population and locus. N, sample size; A, number of alleles per locus; Ar, allelic richness; PA, number of private alleles; PAAr, allelic richness of private alleles; H_O, observed heterozygosity; H_E, expected heterozygosity; F_{IS}, inbreeding coefficient.

Table S5. Estimates of genetic diversity for each of the four *Calotriton asper* populations and loci used in this study. N, sample size; A, number of alleles per locus; H_O, observed heterozygosity; H_E, expected heterozygosity; F_{IS}, inbreeding coefficient. None of the F_{IS} values are statistical significant after Bonferroni correction.

Table S6. Results of the Wilcoxon signed-rank test for the comparison of genetic diversity estimates in terms of differences in heterozygosity estimates (H_E and H_O) and number of alleles per locus (A) between *C. arnoldi* and the four *C. asper* populations. In bold are the significant *p*-value after Bonferroni correction for multiple comparisons.

Table S7. Values used in isolation by distance (IBD) analysis. Measure of genetic differentiation F_{ST} /(1- F_{ST}) below the diagonal; logarithmic geographic distances in km above the diagonal.

Table S8. Recent migration rate estimations between *Calotriton arnoldi* populations within eastern and western sectors**.**

Table S9. Highest posterior probabilities for the demographic parameters inferred with MSVAR. N_0= current effective population size, N_t= ancestral effective population size,

1056 t= time of the change from N_0 to N_t. HPD Low and HPD Up are the lower and upper
1057 highest posterior density interval, respectively. Values in the table are in log(10) scale,
1058 e.g. 2 corresponds to 100 and 4 to 10,000.

1059 Figure 1. A, The distribution range of the Montseny brook newt, *Calotriton arnoldi*.
1060 Populations located in the eastern sector and in the western sector are separated by the
1061 Tordera river valley (Valbuena-Ureña *et al*. 2013). All localities have been sampled for
1062 this study. Shade indicates the actual distribution range of *C. asper*. Locations of the *C.*
1063 *asper* populations used in this study are also shown (ACH: Ibón de Acherito; BAS:
1064 Bassies; IRA: Irati; PER: Ibón de Perramó; VAL: Barranco de Valdragás). B, Bayesian
1065 Inference tree of *Calotriton* inferred using BEAST with the concatenated datasets. A list
1066 of details of all the specimens is presented in Supplementary Table S1. Black-filled
1067 circle indicates pp > 0.95 in the BEAST analysis. Ages of some relevant nodes are
1068 shown by the nodes in with the 95% HPD underneath between square brackets.

1069 Figure 2. A, Results of Bayesian clustering and individual assignment analysis obtained
1070 with STRUCTURE after running the program with all populations (above) and by
1071 sector (below); vertical bars delimit sampling locations. B, inference for the best value
1072 of K based on the ΔK method among runs for all populations and by sector.

1073 Figure 3. Demographic analysis using MSVAR. For populations A1 to A3 and B1 to
1074 B3, their current effective population size is shown (plots A and B), the ancestral
1075 effective population size before the bottleneck (plots C and D), and the time of the
1076 bottleneck (plots E and F). The posterior distributions of each parameter for the A
1077 populations are shown in shades of dark grey, and for the B populations in shades of
1078 light grey. For each population three distributions are shown for each parameter, as each

population was analyzed using three alternative priors. The x-axis is in log(10) scale, for example, 2 represents 100, and 4 represents 10,000.

Figure S1. Population structure based on factorial correspondence analysis of all populations. Each square represents an individual multilocus genotype, colored according to the location from where it was sampled.

Figure S2. Isolation by distance between populations. Blue symbols represent between sectors comparisons; red and black symbols represent between populations comparisons of eastern and western sectors, respectively.

Figure S3. Distribution of ratios of Nt/N0 for each population. For each population three distributions are shown representing the ratio of the ancestral effective population size (Nt) divided by the current effective population size (N0). Under a demographically stable population, the effective population size should be centered around 1 (i.e. Nt/N0 ~1), however, the distributions for each of the three analyses for the populations show values larger than 1 — indicative of a decrease in effective population size consistent with a bottleneck.

Figure S4. Mean within-population pairwise relatedness values (r_{qg}) between populations of eastern (A) and western (B) sectors. Red bars represent the upper (U) and lower (L) confidence intervals with 95 % confidence with a null distribution generated with 999 permutations. Blue bars represent the observed kinship mean conducted with 999 bootstraps.

	Grouping	N	A	Ar	PA	PAAr	H_O
C. arnoldi	Population						
	A1	23	4.167	4.167	7	0.311	0.545
	A2	27	4.042	3.954	5	0.214	0.526
	A3	27	4.292	4.222	5	0.215	0.560
	B1	25	3.542	3.500	3	0.137	0.467
	B2	28	2.917	2.860	2	0.087	0.371
	B3	26	1.792	1.768	2	0.079	0.230
	B4	4	2.333	-	0	-	0.438
	Clusters						
	Eastern	77	4.167	4.112	75	3.157	0.544
	A1-A2	50	4.099	4.052	19	0.746	0.535
	Western	83	2.724	2.703	38	1.646	0.359
	B1-B2-B4	57	3.150	3.162	19	0.750	0.418
C. asper	Population						
	Ibón de Perramó	48	3.947	4.210	19	0.710	0.438
	Barranco de Valdragás	39	6.000	6.010	18	0.770	0.641
	Ibón de Acherito	40	5.895	5.940	18	0.520	0.593
	Bassies	162	4.071	5.690	33	1.130	0.500

H_E	F_{IS}
0.538	0.017
0.516	-0.015
0.559	-0.007
0.469	-0.005
0.380	0.028
0.197	-0.121
0.433	-0.023
0.538	**0.090**
0.526	0.029
0.352	**0.184**
0.423	**0.073**
0.444	0.025
0.619	-0.022
0.588	0.005
0.558	0.107

F_{ST}/D	A1	A2	A3	B1	B2	B3	B4
A1	-	0.131	0.243	0.814	0.816	0.852	0.782
A2	0.086	-	0.299	0.855	0.868	0.877	0.822
A3	0.151	0.178	-	0.806	0.801	0.858	0.762
B1	0.457	0.473	0.443	-	0.100	0.249	0.122
B2	0.509	0.524	0.491	0.096	-	0.248	0.146
B3	0.614	0.617	0.599	0.336	0.372	-	0.305
B4	0.443	0.460	0.419	0.109	0.145	0.488	-

		LDNe			OneSamp		
	Population	N_e	95% CIs		N_e	95% CIs	
C. arnoldi	A1	342.30	77.00	infinite	27.65	24.51	34.81
	A2	49.40	32.20	93.20	33.94	29.94	41.89
	A3	142.10	61.80	infinite	36.85	33.33	43.20
	B1	55.80	34.10	126.40	31.59	27.77	40.69
	B2	62.20	27.50	15091.10	36.39	30.46	53.44
	B3	7.30	2.40	21.70	14.97	12.61	19.61
	B4	infinite	infinite	infinite	5.54	4.87	6.64
	Clusters						
	A1-A2	44.50	36.00	56.50	85.95	66.52	127.10
	B1-B2-B4	30.00	23.60	39.00	80.14	55.44	157.01
C. asper	Population						
	Ibón de Perramó	349.80	100.30	infinite	42.80	33.96	62.07
	Barranco de Valdragás	1293.00	201.40	infinite	41.41	35.29	58.22
	Ibón de Acherito	172.80	89.50	1078.90	60.80	46.42	99.78
	Bassies	92.00	61.90	149.50	28.73	21.65	41.06

COLONY			Relationship			
N_e	95% CIs		Unrelated	Half Siblings	Full Siblings	Parent Offspring
46.00	26.00	90.00	91.70	7.51	0.40	0.40
40.00	25.00	71.00	90.31	7.12	0.85	1.71
44.00	28.00	80.00	91.17	7.98	0.28	0.57
35.00	20.00	68.00	86.33	12.00	0.67	1.00
31.00	18.00	57.00	81.75	13.23	1.85	3.17
13.00	7.00	30.00	68.31	8.00	12.31	11.38
-	-	-	100	-	-	-
60.00	41.00	92.00	84.16	14.37	0.57	0.90
42.00	27.00	66.00	80.89	15.91	1.50	1.69
40.00	26.00	65.00	84.13	12.68	1.60	1.60
58.00	37.00	98.00	90.69	8.50	0.40	0.40
68.00	44.00	111.00	88.85	9.62	0.51	1.03
72.00	53.00	100.00	78.02	16.10	3.57	2.31

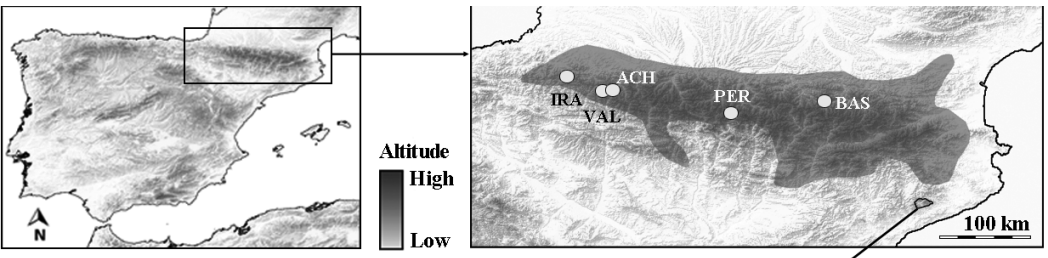
Altitude
High
Low
N
IRA
ACH
VAL
PER
BAS
100 km

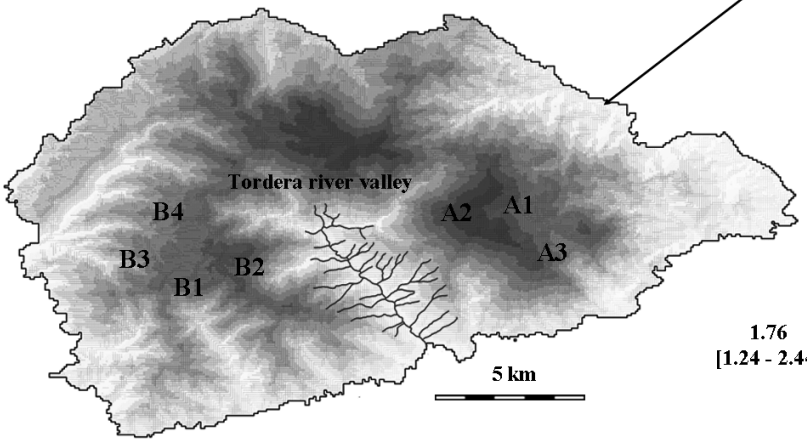
Tordera river valley
B4
B3
B2
B1
A2
A1
A3
5 km

A

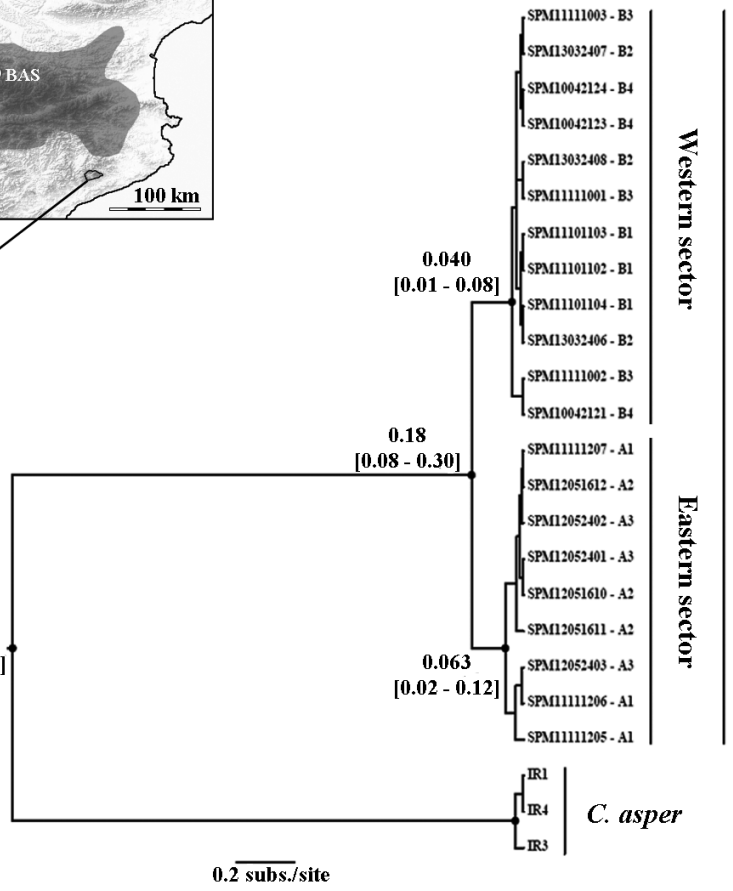
SPM11111003 - B3
SPM13032407 - B2
SPM10042124 - B4
SPM10042123 - B4
SPM13032408 - B2
SPM11111001 - B3
SPM11101103 - B1
SPM11101102 - B1
SPM11101104 - B1
SPM13032406 - B2
SPM11111002 - B3
SPM10042121 - B4
SPM11111207 - A1
SPM12051612 - A2
SPM12052402 - A3
SPM12052401 - A3
SPM12051610 - A2
SPM12051611 - A2
SPM12052403 - A3
SPM11111206 - A1
SPM11111205 - A1
IR1
IR4
IR3
0.040
[0.01 - 0.08]
0.18
[0.08 - 0.30]
1.76
[1.24 - 2.44]
0.063
[0.02 - 0.12]
Western sector
Eastern sector
Calotriton arnoldi
C. asper
0.2 subs./site

B

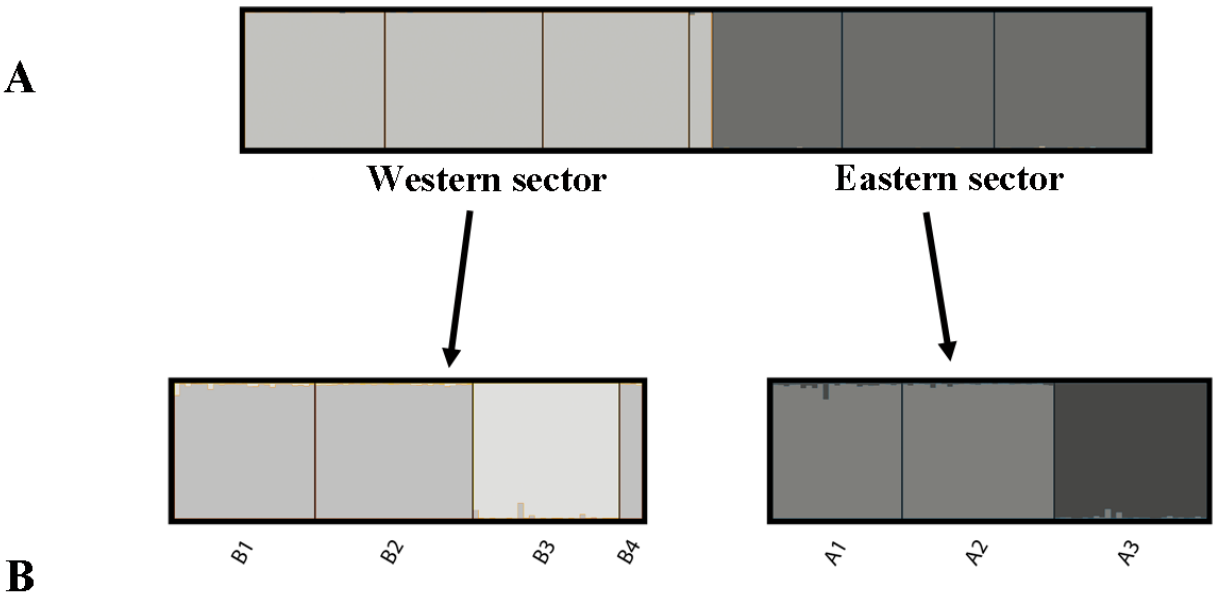
A
Western sector
Eastern sector
B1
B2
B3
B4
A1
A2
A3

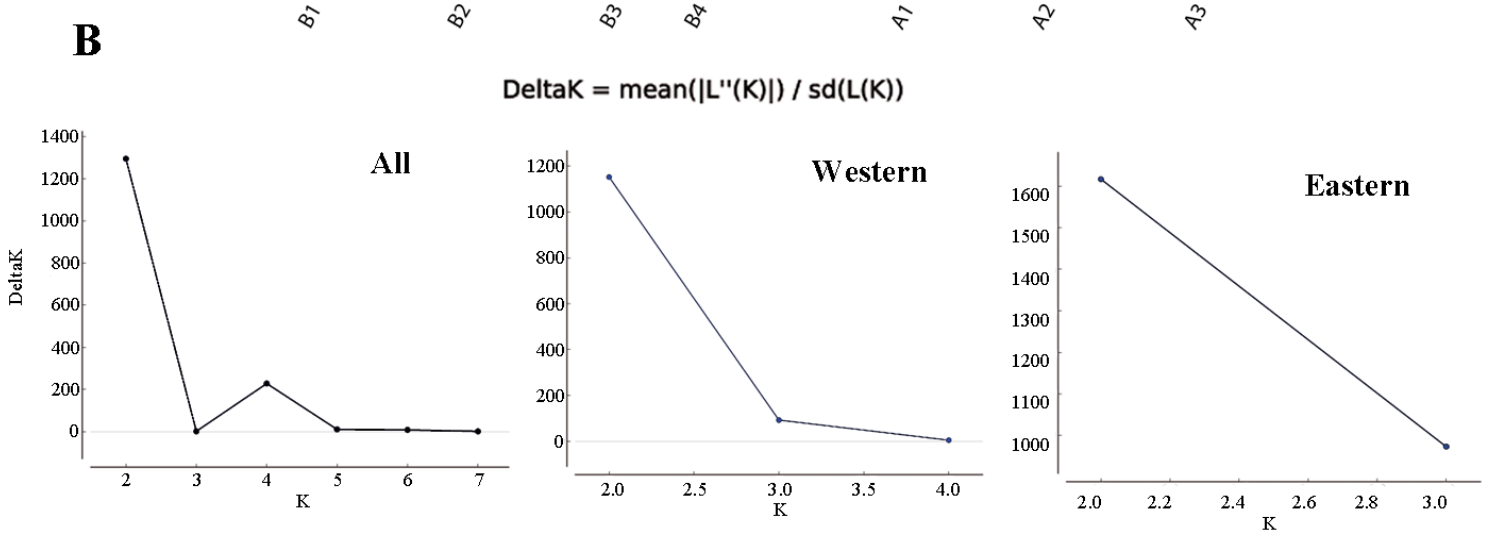
B
DeltaK = mean(|L''(K)|) / sd(L(K))
All
Western
Eastern
DeltaK
K

A

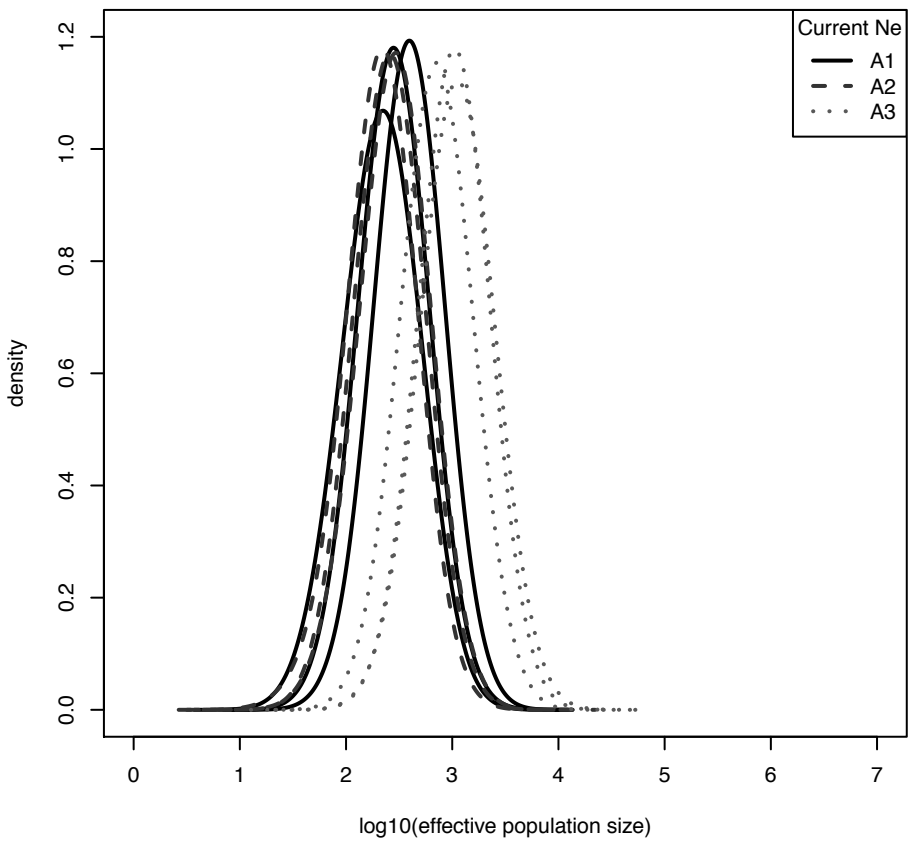
Current Ne
A1
A2
A3
density
log10(effective population size)

B

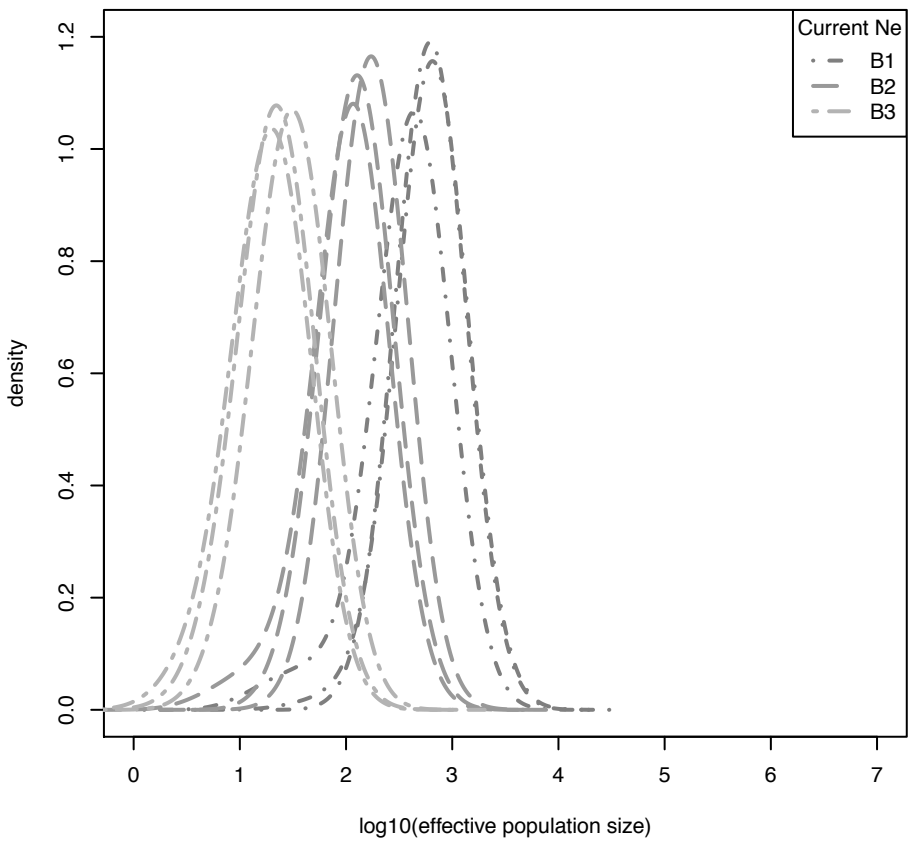
Current Ne
B1
B2
B3
density
log10(effective population size)

C

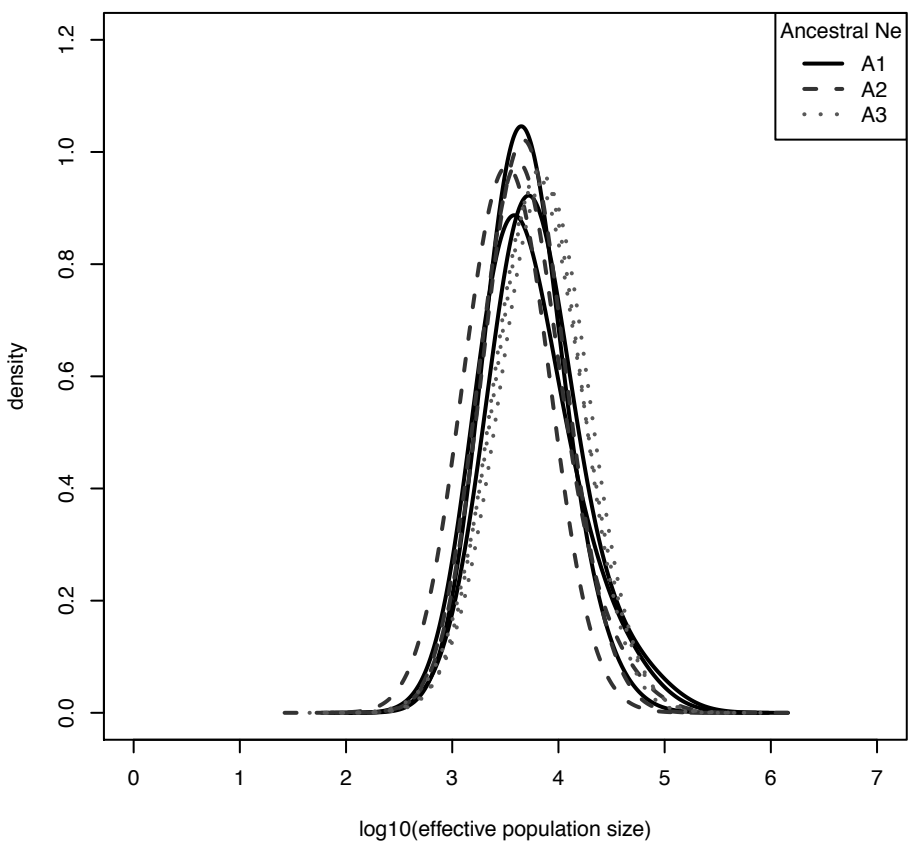
Ancestral Ne
A1
A2
A3
density
log10(effective population size)

D

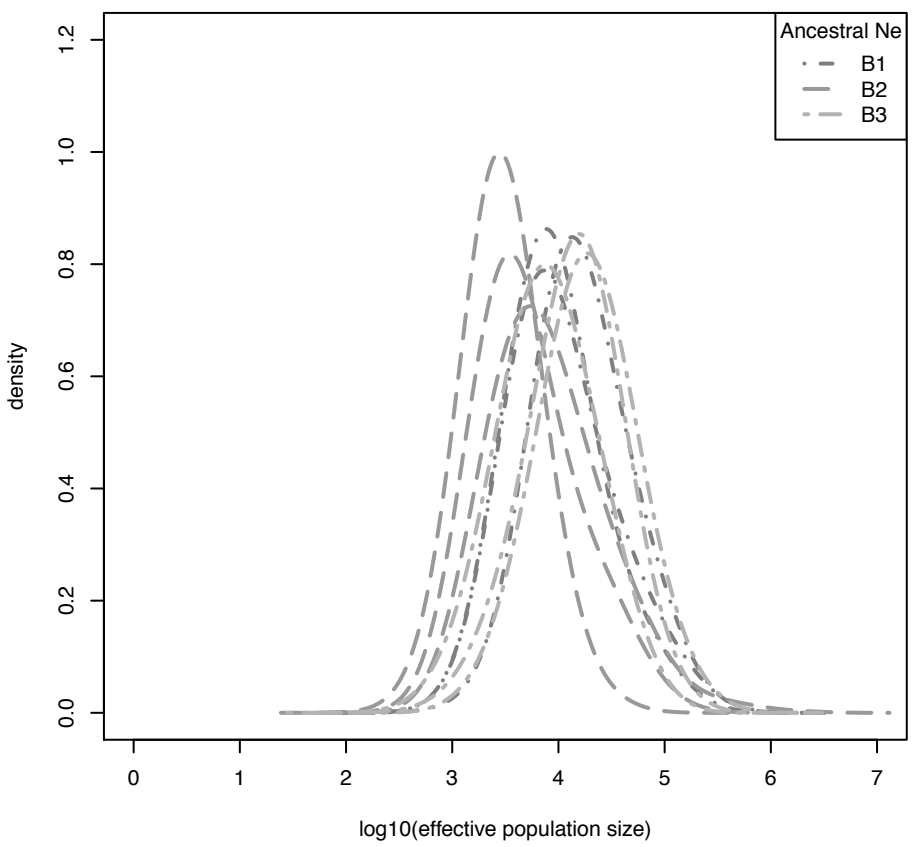
Ancestral Ne
B1
B2
B3
density
log10(effective population size)

E

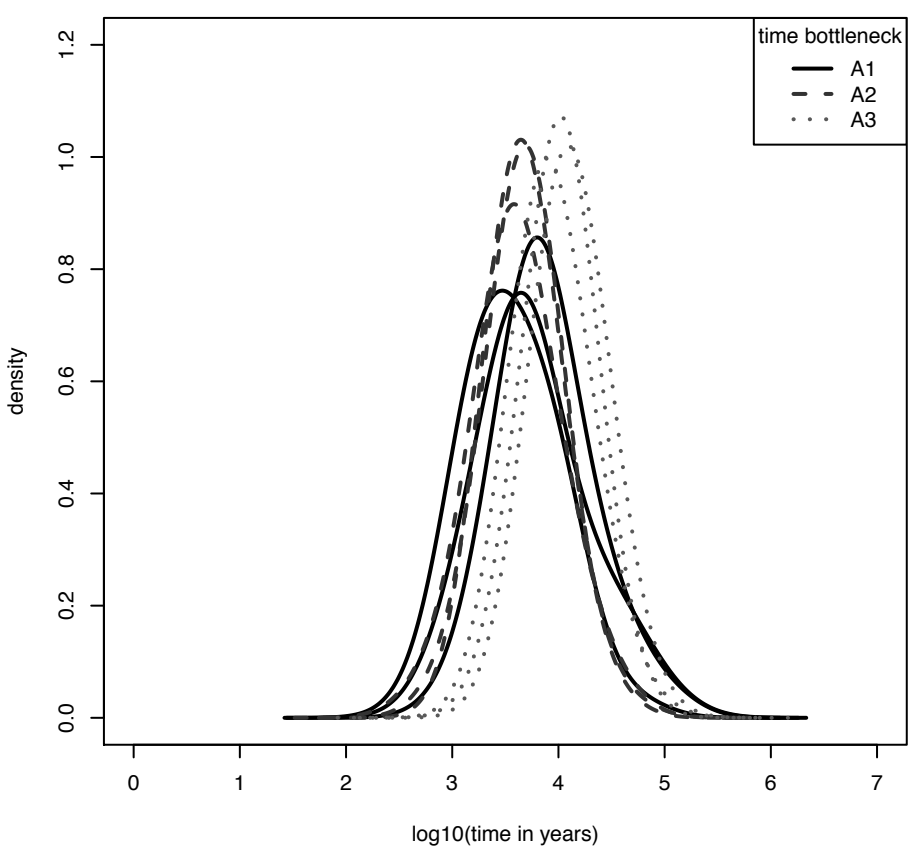
time bottleneck
A1
A2
A3
density
log10(time in years)

F

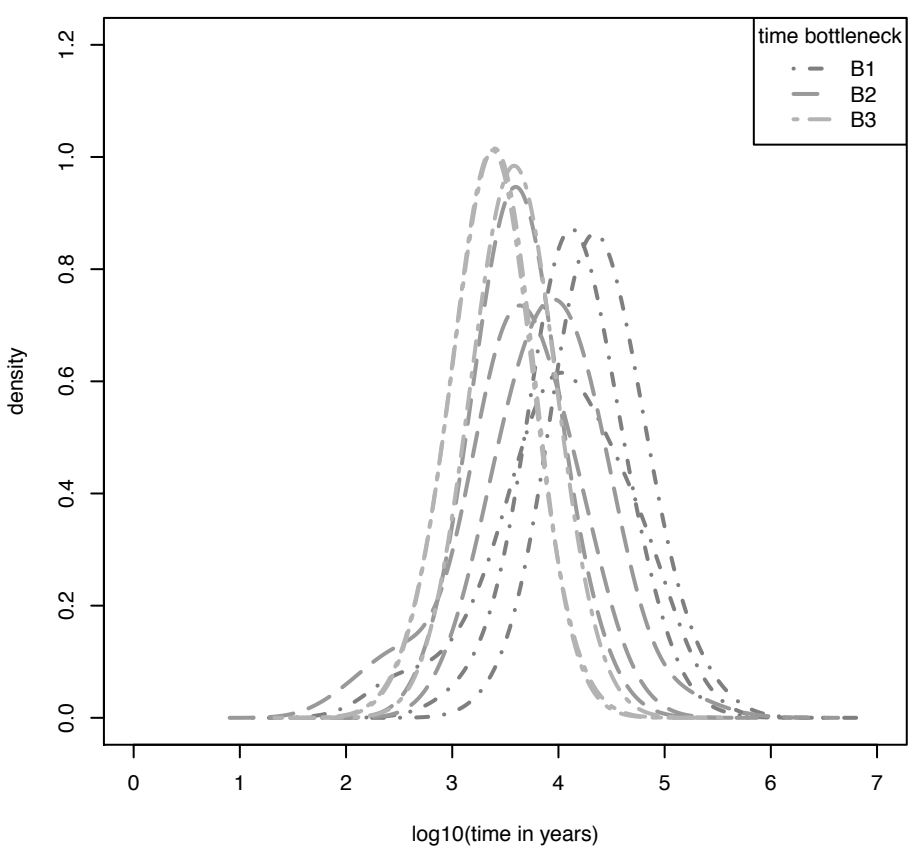
time bottleneck
B1
B2
B3
density
log10(time in years)